Research report

BYTEC

Background theory for a numerical model for Sandwich beams

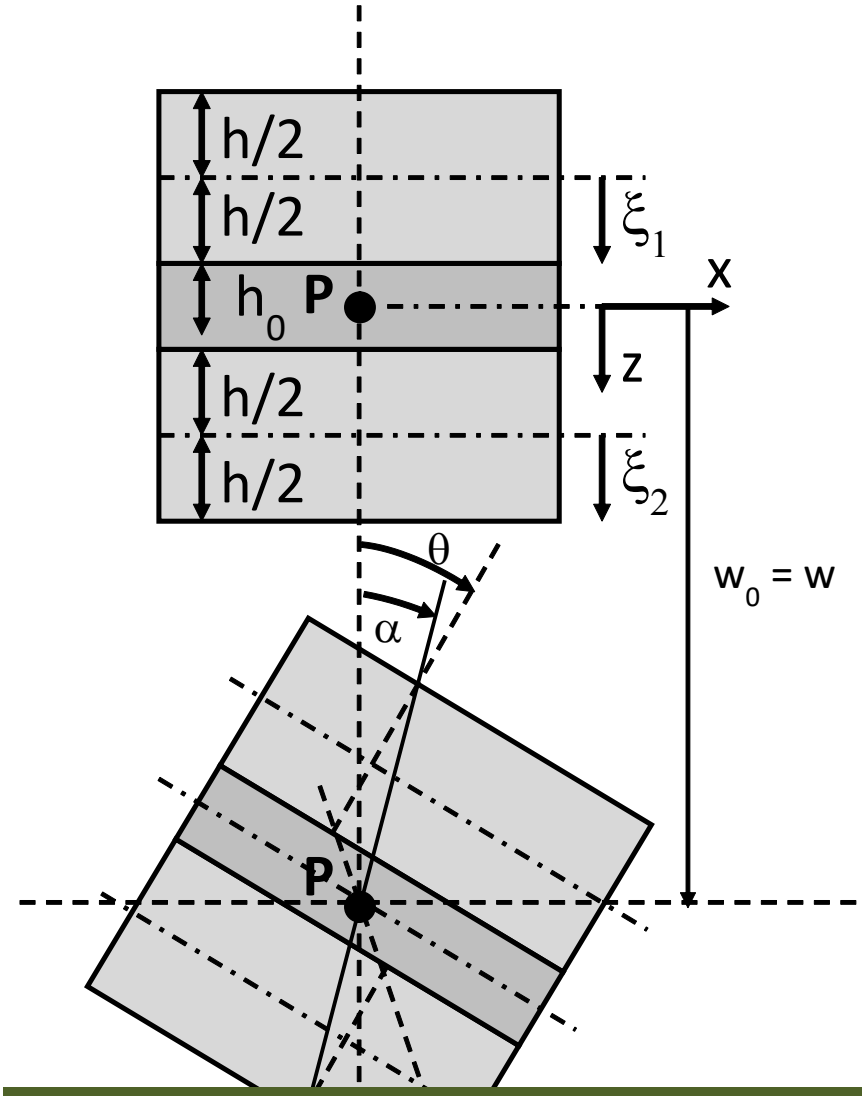

Report date: 4 May 2026 Hugo Sol

Contents

1 Abstract

This report describes a one-dimensional numerical beam model of a triplex sandwich beam. The triplex sandwich beam consists of a laminate of two glass layers bonded together by a polymer interlayer. For the numerical modeling, the central line of the triplex sandwich beam is divided into a series of nodal points. Each node has two degrees of freedom (abbreviated “d.o.f”): a transverse displacement w and a rotation angle α. All section forces, deformations, stresses and strains in the different layers of the laminate are expressed as a function of these two degrees of freedom.

The numerical model will be used for the identification of the transverse shear modulus of the polymer layer based on measured resonance frequencies of a test beam. The resonance frequencies of a free-free suspended sandwich beam will be measured using an impulse excitation technique. The vibration amplitudes of the test beam are very small. This allows assuming a small deformation theory and linear material behavior in the numerical model of the sandwich beam.

The tangents delta of the loss modulus can be identified with the measured damping ratio of the test beam, based on an analysis of the potential energy contributions of the different layers.

2 Introduction

Safety glass consists of a laminate of two glass layers bonded together by a polymeric interlayer. It is used as windshields in the automotive industry and also widely used as architectural glazing. The polymeric layer increases the damping value, provides a thermal isolation and keeps the shards of broken glass fragments together in case of failure.

There are three main commercial polymeric films, each one showing peculiar characteristics: Polyvinyl Butyral (PVB), Ethylene Vinyl Acetate (EVA), and Sentry Glass (SG). Pure PVB, a polyvinyl acetate, is stiff and brittle, but addition of softeners imparts plasticity and toughness, though influencing adhesion-strength, elasticity, water-absorbability and dependence on temperature (glass transition temperature of the order of 20–25 °C). Depending on the composition, the properties of EVA, a polyolefin, vary from partial crystalline and thermoplastic to amorphous and rubber-like, but an increased quantity of vinyl acetate improves strength and ultimate elongation, though decreasing melting temperature: when used as interlayers in laminated glass, modified EVAs are employed with mechanical properties similar to PVB. A somehow innovative material is SG, an ionoplast polymer that, when compared with PVB, presents higher stiffness (>100 times PVB), strength (>5 times PVB) and higher resistance to temperature.

The elastic Young's and transverse shear modulus of the polymeric layer are much lower than the elastic Young's and shear modulus of glass. This mismatch prevents the use of the classical laminate theory (CLT) to describe the mechanical behavior of the sandwich laminate. The shearing behavior of the polymeric layer must be considered. The shearing behavior is mainly governed by the laminate configuration and the transverse shear modulus of the polymeric layer.

For the elastic modeling, no distinction has to be made for what the type of glass is concerned, because all treatments (annealing, heat strengthening, heat or chemical tempering) affect the ultimate strength and the type of rupture (size of

resulting shards) but nearly not the value of the elastic moduli (Young's modulus with a value of 70 GPa and Poisson ratio of value 0.2).

This report describes a method to reduce the 3-dimensional body of a symmetric triplex glass beam into a one-dimensional beam. The deformation of the one-dimensional beam will be described solely by the deformation of the central line of the laminate.

The deformation of the central line will be expressed as a function of two independent degrees of freedom, being the transverse displacement w and the global rotation angle Alfa in each point. All section forces, deformations, stresses and strains in the different layers of the laminate will be expressed as a function of these two degrees of freedom.

The numerical model will be used for the identification of the transverse shear modulus of the polymer layer, based on measured resonance frequencies of a test beam. The resonance frequencies of a free-free suspended sandwich beam will be measured using an impulse excitation technique. The vibration amplitudes of the test beam will be very small. This will allow assuming a small deformation theory and linear material behavior in the numerical model of the sandwich beam.

The tangents delta of the loss modulus can be identified with the measured damping ratio of the test beam, based on an analysis of the potential energy contributions of the different layers.

3 Mechanical model of a symmetric laminated glass PVB sandwich beam

3.1 Model Assumptions

The mechanics of the laminated glass beam will be described in this report according to a right-handed orthogonal reference frame (x, y, z). The section forces are described as the exerted action of the right part of the section on the left part of the section. Positive rotation angles and moments comply with the right-hand rule. Forces, stresses, strains and displacements are positive along the positive axes. All deformations and strains are assumed to remain infinitely small. The elastic and shear modulus of the glass and polymer are assumed to be constants. The deformation mechanism can hence be described using a linear theory.

Figure 3.1.1 describes the geometry of the symmetric triplex glass beam.

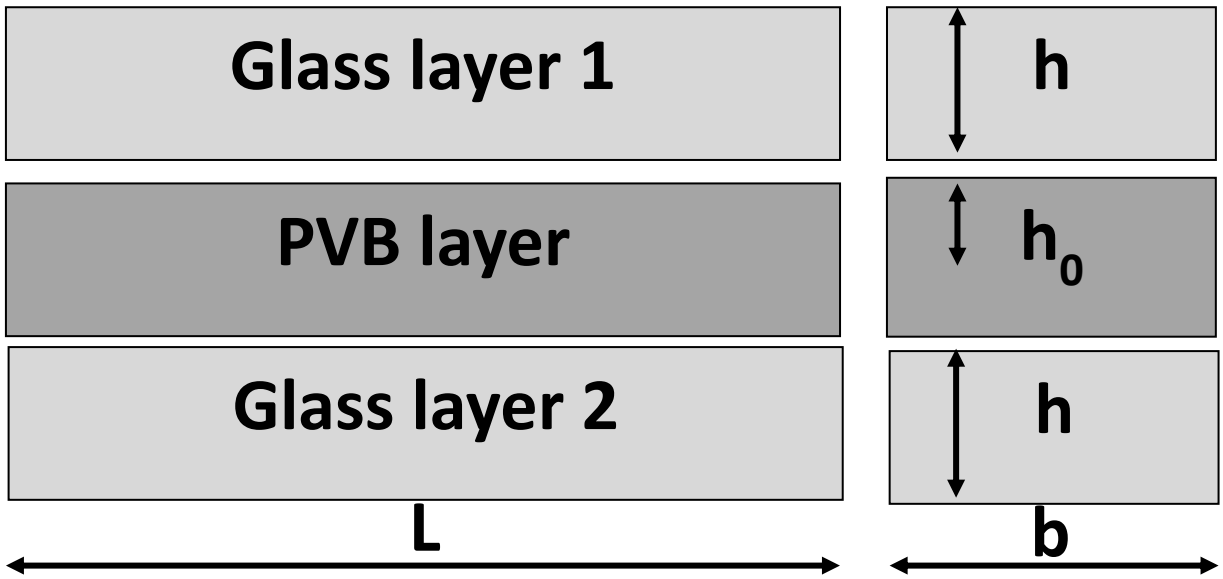

Figure 3.1.1. Geometry of a triplex glass beam and cross section.

The laminated glass beam has a length of L and a width b. The height h is assumed equal for both glass layers. The polymer layer is situated between both glass layers and has a height h_0.

3.2 Deformation and section forces in the laminated sandwich beam

3.2.1 Deformation in the laminated sandwich beam

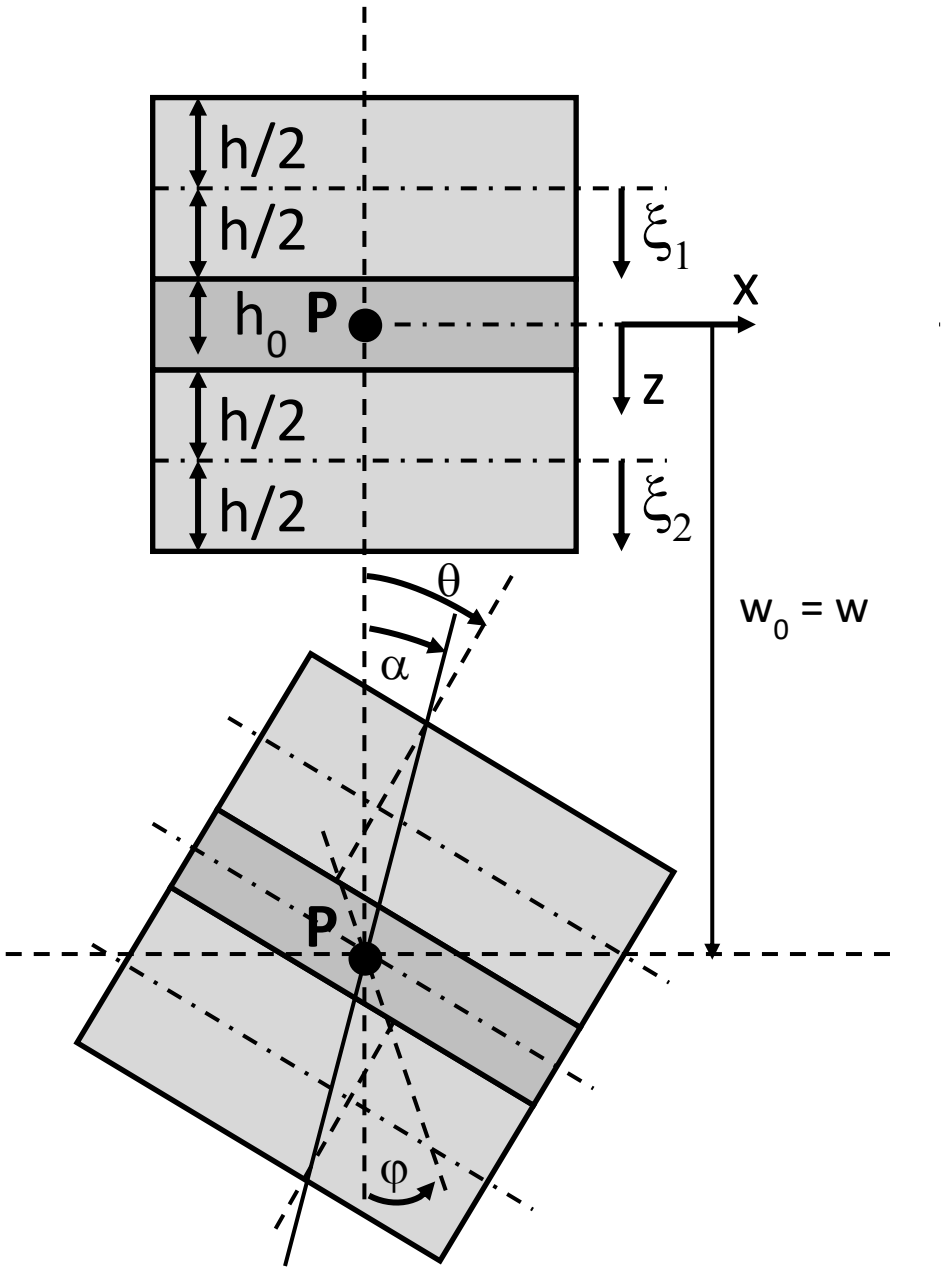

Figure 3.2.1.1. Deformation of the triplex glass beam (positive y-axe coming out of the paper)

Figure 3.2.1.1 shows the deformation of a section of the laminated glass beam.

Figure 3.2.1.1. shows what happens with the cross-sections of the sandwich beam during bending. The straight normal of the laminate layers is converted

into broken straight lines. The normal of the upper and lower glass layers remain straight after the deformation. The middle layer is sheared.

The transverse displacement *w(x, z)* of an arbitrary point of the section is assumed to be equal to the transverse displacement of point P on the central line of the PVB layer.

$$w(x,z) = w_0(x) = w(x) \tag{1}$$

This assumption is acceptable for infinite small deformations. The assumption implies incompressibility of the PVB layer.

For each glass layer, the normal is assumed to remain straight and perpendicular to the central line of the glass layer. The rotation angle θ of the normal after deformation is the same for both glass layers. In figure 3.2.1.1 the shown rotation angle around the y-axis θ has a negative value according to the right-hand rule (the positive y-axis is coming out of the paper)

It is assumed that the displacement field of a section shows no discontinuities at the boundaries between the glass layers and the polymer layer (perfect adhesion of the layers). This is accomplished by shearing the polymer layer with a shear angle φ. The section in the polymer layer is assumed to have a constant rotation angle φ, causing shear deformation. In figure 3.2.1.1 the shown rotation angle φ has a positive value according to the right-hand rule.

The angle α describes the global rotation of a section of the laminate considered as a homogeneous beam. In figure 3.2.1.1 the shown rotation angle α has a negative value according to the right-hand rule.

3.2.2 Deformation and section forces in the glass layers

Figure 3.2.2.1 shows the deformation, stresses and section forces in a section of the glass layers.

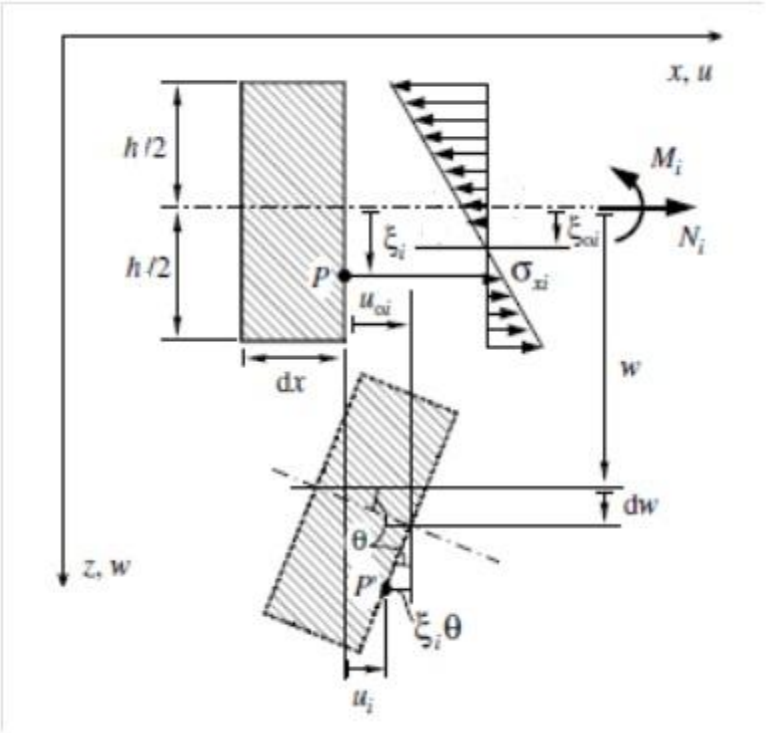

Figure 3.2.2.1 Deformation, stresses and section forces of the glass layers

Although the global laminate deformation cannot be described by the CLT, it is assumed that the normal of each individual glass layer remains straight and perpendicular on its central axe after deformation. The individual glass layers hence behave according to the Euler-Bernoulli bending theory of thin beams.

The bending moment M_i induces the rotation $\theta(x)$ of the glass layer i. The normal force N_i induces a normal displacement $u_{Oi}(x)$. The displacements $u_i(x,\xi_i)$, normal strains $\varepsilon_i(x,\xi_i)$ and normal stresses $\sigma_{xi}(x,\xi_i)$ of an arbitrary point P of glass layer i can be written as function of the local coordinate ξ_i:

$$\begin{cases} u_i(x,\xi_i) = u_{Oi}(x) + \xi_i\theta(x) \\ \varepsilon_i(x,\xi_i) = \dfrac{\partial u_i}{\partial x} = \varepsilon_{Oi}(x) + \xi_i \dfrac{\partial\theta(x)}{\partial x} \\ \sigma_{xi}(x,\xi_i) = E\varepsilon_i(x,\xi_1) = E\varepsilon_{Oi}(x) + \xi_i E\left(\dfrac{\partial\theta(x)}{\partial x}\right) \end{cases} \quad (2)$$

The position of the neutral axis in the glass layer is ξ_{i0}.

The bending rotation angle $\theta(x)$ shown in figure 3.2.2.1 can be expressed as a function of w(x):

$$\theta(x) = -\frac{\partial w(x)}{\partial x} \tag{3}$$

The displacements, strains and stresses hence can be rewritten as function of derivatives of w(x):

$$\begin{cases} u_i(x,\xi_i) = u_{Oi}(x) - \xi_i \dfrac{\partial w(x)}{\partial x} \\ \varepsilon_i(x,\xi_i) = \varepsilon_{Oi}(x) - \xi_i \dfrac{\partial^2 w(x)}{\partial x^2} \\ \sigma_{xi}(x,\xi_i) = E\varepsilon_{Oi}(x) - \xi_i E \dfrac{\partial^2 w(x)}{\partial x^2} \end{cases} \tag{4}$$

The normal section force N_i is:

$$N_i(x) = \int_{-\frac{h}{2}}^{\frac{h}{2}} \sigma_{xi} b d\xi_i = Ebh\,\varepsilon_{Oi}(x) = Ebh\frac{\partial u_{0i}}{\partial x} \tag{5}$$

The bending moment of the section M_i is:

$$M_i(x) = \int_{-\frac{h}{2}}^{\frac{h}{2}} \sigma_{xi}\xi_i b d\xi_i = -E\frac{bh^3}{12}\frac{\partial^2 w}{\partial x^2} \tag{6}$$

The normal forces N_i in both upper and lower glass layers act as a couple of forces inducing a moment M_0.

$$M_0(x) = -\mathrm{N}(\mathrm{h} + \mathrm{h}_0) \tag{7}$$

3.2.3 Deformation and section forces in the polymer layer

The polymeric interlayer affects the elastic stiffness of the laminated beam because it allows the transfer of shear stresses among both glass plies by a relative sliding due to the deformation of the polymer. In general, the degree of coupling of two glass layers depends upon the shear stiffness of the polymeric interlayer.

It is assumed that the shear strain and stress in the polymeric layer are constant through its thickness. The total shear angle γ is composed of two rotation angles, the "forced" bending angle θ and shear angle φ (see figure 3.2.3.1).

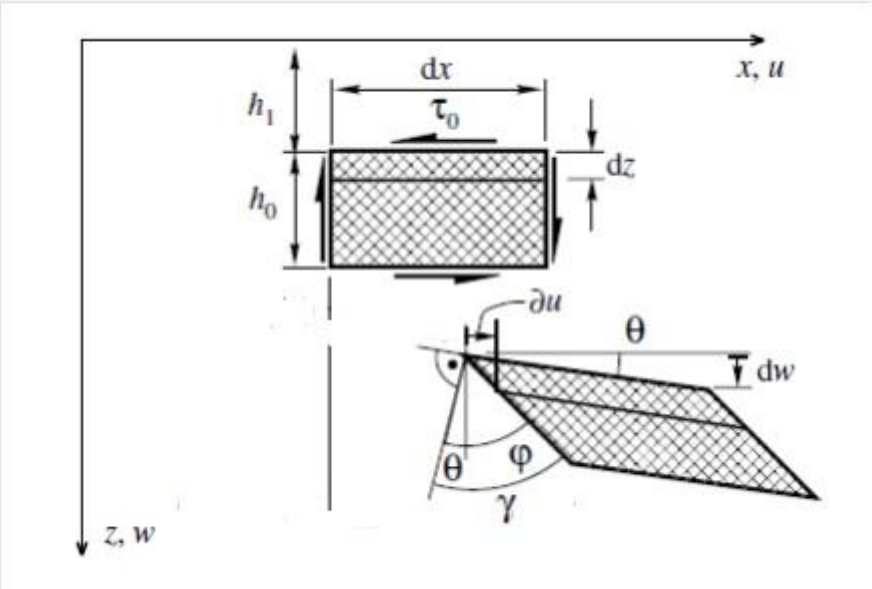

Figure 3.2.3.1. Deformation, stresses and section forces of the polymeric intermediate layer

The shear angle φ is assumed to be constant in the polymer layer and can be computed as:

$$\varphi = \frac{\partial u}{\partial z} = \frac{u_1(x,-\frac{h}{2})}{-h_0/2} = \frac{u_2(x,\frac{h}{2})}{h_0/2} \tag{8}$$

The total shear angle γ is:

$$\gamma(x) = \varphi - \theta = \frac{\partial u}{\partial z} + \frac{\partial w}{\partial x} \tag{9}$$

The shear stress is found by multiplying the shear strain with the transverse shear modulus G_0 of the polymer:

$$\tau(\mathrm{x}) = \gamma(x)\mathrm{G}_0 \tag{10}$$

The normal stresses of the intermediate layer due to bending are small as compared to the bending stresses in the glass layers because the Young's modulus E_0 of the polymer is typically small as compared to the Young's modulus of glass.

$$M_{inter}(x) = \int_{-\frac{h_0}{2}}^{\frac{h_0}{2}} \sigma_x \mathrm{z} b d\mathrm{z} = E_0 \frac{b{h_0}^3}{12} \frac{\partial^2 w}{\partial x^2} \tag{11}$$

The bending moment M_{inter} is consequently small as compared to M_1, M_2 and M_0. If E_0 is small, the intermediate layer will mainly contribute through shear not through bending.

3.3 Potential energy of the stressed laminated glass beam

The potential energy V of the laminated sandwich beam receives contributions from the stresses and strains in the glass layers and the stresses and strains in the intermediate polymer layer.

$$\mathrm{V} = \mathrm{V}_{\mathrm{glass}} + \mathrm{V}_{\mathrm{polymer}} \tag{12}$$

The glass layers contribute to the potential energy by the bending mechanism and the normal forces.

$$\mathrm{V}_{\mathrm{glass}} = \mathrm{V}_{\mathrm{bending}} + \mathrm{V}_{\mathrm{normal\ forces}} \tag{13}$$

By integration over the length L of the beam (the origin of the x-axis is taken in the middle of the beam), the potential energy of one glass layer can be computed as:

$$\mathrm{V}_{\mathrm{glass}} = \frac{1}{2}\int_{-\mathrm{L}/2}^{\mathrm{L}/2} \mathrm{E}\frac{bh^3}{12}\left(\frac{\partial\theta}{\partial \mathrm{x}}\right)^2 d\mathrm{x} + \frac{1}{2}\int_{-\mathrm{L}/2}^{\mathrm{L}/2} \mathrm{E}bh\left(\frac{\partial u_0}{\partial \mathrm{x}}\right)^2 d\mathrm{x} \tag{14}$$

By integration over the length L of the beam, the potential energy of the polymeric intermediate layer can be computed as:

$$V_{polymer} = \frac{1}{2}\int_{-L/2}^{L/2} h_0 b G_0(\gamma)^2 dx + \frac{1}{2}\int_{-L/2}^{L/2} E_0 \frac{b{h_0}^3}{12}\left(\frac{\partial\theta}{\partial x}\right)^2 dx \quad (15)$$

The potential energy V of the laminated beam (2 glass layers + 1 polymer layer) hence is:

$$V = \int_{-L/2}^{L/2} E\frac{bh^3}{12}\left(\frac{\partial\theta}{\partial x}\right)^2 dx + \int_{-L/2}^{L/2} Ebh\left(\frac{\partial u_0}{\partial x}\right)^2 dx + \frac{1}{2}\int_{-L/2}^{L/2} h_0 b G_0(\gamma)^2 dx + \frac{1}{2}\int_{-L/2}^{L/2} E_0 \frac{b{h_0}^3}{12}\left(\frac{\partial\theta}{\partial x}\right)^2 dx \quad (16)$$

3.4 Extreme cases

3.4.1 Pure bending of the laminate

If the Young's modulus of the polymer layer becomes equal to the Young's modulus of the glass, then the shear angle φ becomes equal to the bending rotation angle θ and the global rotation angle α. The total shear angle γ becomes zero (see figure 3.4.1.1)

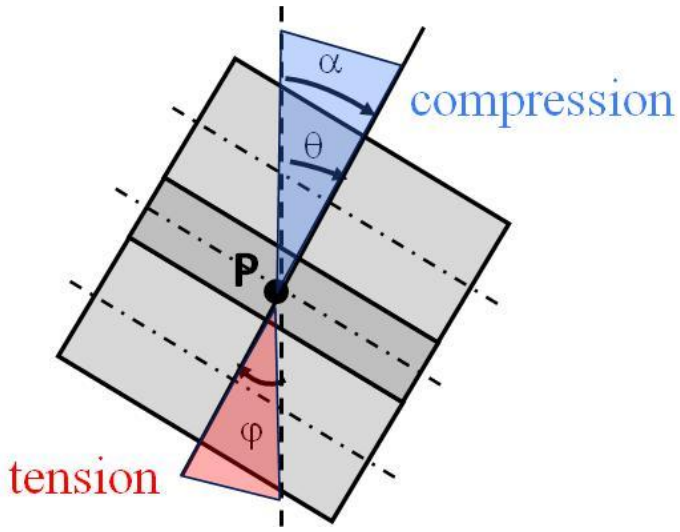

Figure 3.4.1.1. Monolithic bending of the laminated beam

$$\varphi = \theta = \alpha$$

and

$$\gamma(x) = \varphi - \theta = 0 \quad (17)$$

The laminated beam behaves as a monolith glass beam with thickness $2h+h_0$ and thus exhibit maximal stiffness. The bending stiffness can be computed as:

$$(EI)_{monolith} = E\frac{b(2h+h_0)^3}{12} \tag{18}$$

3.4.2 Independent bending of the glass layers

The axial displacement of the central line of the glass layers becomes zero. The axial displacement at the interface line can be computed relative to the glass layer and relative to the polymer layer.

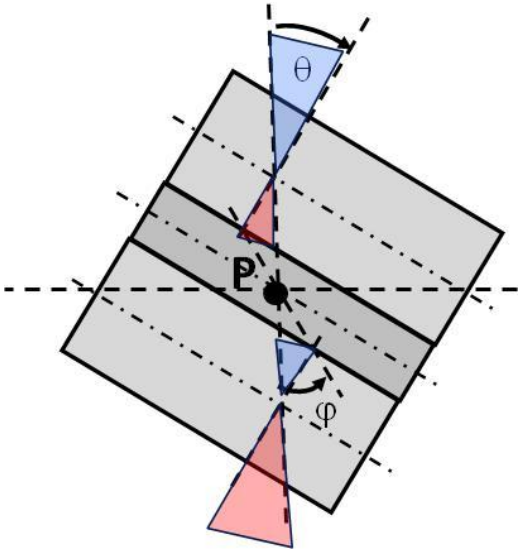

Figure 3.4.2.1. Bending of the laminated beam as two separate glass layers

$$\theta\frac{h}{2} = \varphi(-\frac{h_0}{2}) \tag{19}$$

$$\gamma(x) = \varphi - \theta = \varphi(\frac{h+h_0}{h}) \tag{20}$$

The laminated beam behaves as two separate glass layers, spaced with a distance h_0, and thus has minimum stiffness. The total shear angle γ becomes maximal.

The bending stiffness can be computed as:

$$(EI)_{two\ separate\ glass\ beams} = Eb\frac{h^3}{6} \tag{21}$$

3.5 Potential energy expression as a function of selected degrees of freedom

3.5.1 Axial strain in the glass layers expressed as function of the d.o.f.

In figure 3.2.1, it can be observed:

$$u_1\left(x,-\frac{h}{2}\right) = -\alpha(2h + h_0)/2 \tag{22}$$

The displacement at position $\xi_1 = -h/2$ can also be found with (2):

$$u_1\left(x,-\frac{h}{2}\right) = u_{O1}(x) + \frac{h}{2}\frac{\partial w(x)}{\partial x} \tag{23}$$

Thus, u_{01} can be expressed as a function of degrees of freedom w and α:

$$u_{O1}(x) = -\frac{\alpha(2h+h_0)}{2} - \frac{h}{2}\frac{\partial w(x)}{\partial x} \tag{24}$$

Since u_{01} = - u_{02}, the square value of the derivative of u_0 is:

$$\left(\frac{\partial u_O}{\partial x}\right)^2 = \left[\frac{(2h+h_0)}{2}\frac{\partial \alpha}{\partial x} + \frac{h}{2}\frac{\partial^2 w(x)}{\partial x^2}\right]^2 \tag{25}$$

3.5.2 Shear strain in the polymer layer expressed as function of the d.o.f.

The axial displacement in glass layer 1 at the interface position $\xi_1 = h/2$ can be found with (2):

$$u_1\left(x,\frac{h}{2}\right) = u_{O1}(x) - \frac{h}{2}\frac{\partial w(x)}{\partial x} \tag{26}$$

With (23):

$$u_1\left(x,\frac{h}{2}\right) = -\frac{\alpha(2h+h_0)}{2} - h\frac{\partial w(x)}{\partial x} \tag{27}$$

The assumption of continuity of the axial displacement at the interface glass-polymer allows expressing the same axial displacement at the interface as a function of the shear angle in the polymer layer (see figure 3.2.3.1):

$$u_1\left(x,\frac{h}{2}\right) = -\varphi\frac{h_0}{2} \tag{28}$$

Combining (24) and (27) and using (8):

$$\frac{\partial u}{\partial z}\frac{h_0}{2} = \frac{\alpha(2h+h_0)}{2} + h\frac{\partial w(x)}{\partial x} \tag{29}$$

Adding $\frac{\partial w}{\partial x}\frac{h_0}{2}$ to both the left and right hand side:

$$\left(\frac{\partial u}{\partial z} + \frac{\partial w}{\partial x}\right)\frac{h_0}{2} = \frac{\alpha(2h+h_0)}{2} + h\frac{\partial w(x)}{\partial x} + \frac{\partial w}{\partial x}\frac{h_0}{2} \tag{30}$$

With (9):

$$\gamma = \left(\frac{\partial u}{\partial z} + \frac{\partial w}{\partial x}\right) = \frac{\alpha(2h+h_0)}{h_0} + \frac{\partial w(x)}{\partial x}\frac{(2h+h_0)}{h_0} \tag{31}$$

3.5.3 Potential energy V of the laminated beam

The expression for the potential energy V can now be expressed as a function of the selected global degrees of freedom w and α.

(31) and (25) in (15), taking relation (5) into account, yield (32):

$$V = \int_{-L/2}^{L/2} E\frac{bh^3}{12}\left(\frac{\partial^2 w}{\partial x^2}\right)^2 dx + \int_{-L/2}^{L/2} Ebh\left[\frac{(2h+h_0)}{2}\frac{\partial \alpha}{\partial x} + \frac{h}{2}\frac{\partial^2 w}{\partial x^2}\right]^2 dx + \frac{1}{2}\int_{-L/2}^{L/2} h_0 bG_0\left(\frac{\alpha(2h+h_0)}{h_0} + \frac{\partial w}{\partial x}\frac{(2h+h_0)}{h_0}dx\right)^2 + \frac{1}{2}\int_{-L/2}^{L/2} E_0\frac{bh_0{}^3}{12}\left(\frac{\partial^2 w}{\partial x^2}\right)^2 dx \tag{32}$$

This potential energy expression allows deriving the stiffness matrix of a finite element by the Lagrange equations.

3.6 Kinetic energy of the vibrating laminated beam

For the computation of the inertia forces, the contribution of each layer must be evaluated. The translation inertia equals to $\rho A + \rho_0 A_0$ in which ρ is the specific mass of the glass, A is the cross-section area of both glass layers together, ρ_0 is

the specific mass of the polymer and A_0 is the cross-section area of the polymer layer.

The rotation inertia equals to $\rho I + \rho_0 I_0$ in which ρ is the specific mass of the glass, I is the cross section inertia of both glass layers together, ρ_0 is the specific mass of the polymer and I_0 is the cross section inertia of the polymer layer.

The inertia contributions to the kinetic energy come from the translation velocity $\frac{\partial w}{\partial t}$ and the rotation velocity $\frac{\partial \alpha}{\partial t}$ of a beam with constant width b and constant height $2h + h_0$.

$$T = \frac{1}{2}\int_{-L/2}^{L/2}(\rho A + \rho_0 A_0)\left(\frac{\partial w}{\partial t}\right)^2 dx + \frac{1}{2}\int_{-L/2}^{L/2}(\rho I + \rho_0 I_0)\left(\frac{\partial \alpha}{\partial t}\right)^2 dx \quad (33)$$

This kinetic energy expression allows deriving the mass matrix of a finite element by the Lagrange equations.

3.7 External work by external forces

The work done by external forces can have contributions from a distributed load p(x), isolated shear forces Q and isolated bending couples M.

The total potential energy π can be computed as the potential energy generated by the stresses in the deformed laminated beam and the work done by the external forces.

$$\pi = V - \int p(x) w dx - Q.w - M.\alpha \quad (34)$$

4 Formulation of the numerical model

4.1 Discrete model of the central line of the sandwich beam

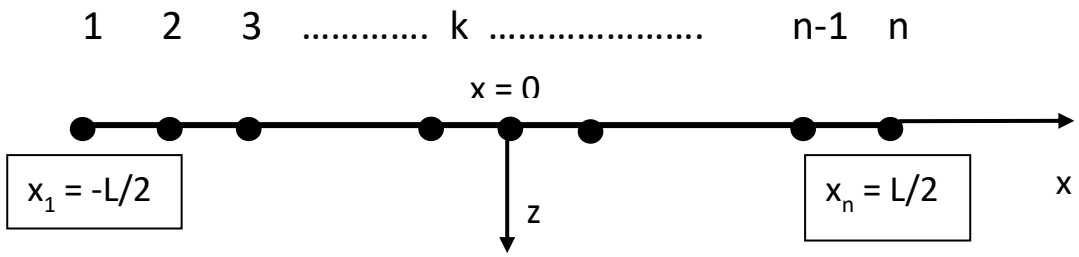

Figure 4.1.1. Discrete numerical model of the laminate beam

The central line of the laminated beam is divided into a regular grid of n equidistant nodal points. The x axis has its origin in the middle of the beam. The value of x in node 1 is –L/2. The value of x in node n is L/2. The value of the degrees of freedom w(x) and α(x) in an arbitrary point x of the central line are expressed as a summation of interpolation functions multiplied with the value of the degrees of freedom in the nodal points. High polynomial Lagrange functions are proposed as interpolation functions.

The Lagrangian interpolation function N associated to node k is:

$$N_k = \frac{(x-x_1)(x-x_2)\ldots(x-x_{k-1})(x-x_{k+1})\ldots(x-x_n)}{(x_k-x_1)(x_k-x_2)\ldots(x_k-x_{k-1})(x_k-x_{k+1})\ldots(x_k-x_n)} \quad (35)$$

It can be verified that the function N_k equals to 1 in node k and equals to zero in all other nodes.

The degrees of freedom of the nodal points can be stored in a displacement column {U}.

$$\{U\} = \begin{Bmatrix} w_1 \\ \alpha_1 \\ \vdots \\ w_n \\ \alpha_n \end{Bmatrix} \quad (36)$$

The two degrees of freedom can be interpolated with the same Lagrangian interpolation function (repeated index means summation, according to the Einstein notation):

$$w(x) = \mathrm{N_j(x)w_j} \qquad \mathrm{j = 1, n} \tag{37}$$

$$\alpha(x) = \mathrm{N_j(x)\alpha_j} \qquad \mathrm{j = 1, n} \tag{38}$$

The numerical model of the laminated beam hence has 2n degrees of freedom.

4.2 The equations of motion of the laminated beam

The equations of motion of a multi degree of freedom system can be derived from Lagrange's equations.

$$\frac{d}{dt}\left(\frac{\partial T}{\partial v}\right) - \frac{\partial T}{\partial U_i} + \frac{\partial V}{\partial U_i} = \mathrm{Q_i} \tag{39}$$

{U} is the column defined in (36), {v} is the velocity column which can be found by taking the time derivative of {U}. {Q} is the column with external local shear forces and bending moments in the nodes.

The kinetic T and potential energy V of a multi degree of freedom system can be expressed in matrix form.

$$T = \frac{1}{2} M_{ij} v_i v_j \tag{40}$$

$$V = \frac{1}{2} K_{ij} U_i U_j \tag{41}$$

M_{ij} is called the mass matrix and K_{ij} is the stiffness matrix of the numerical multi degree of freedom system.

The first term of (39) can now be computed:

$$\frac{\partial T}{\partial v_i} = M_{ij} v_j \tag{42}$$

$$\frac{d}{dt}\left(\frac{\partial T}{\partial v_i}\right) = M_{ij} a_j \tag{43}$$

In which a_i is the column with the acceleration values (time derivative of the column of the velocities v). Since the kinetic energy V is only a function of {v}:

$$\frac{\partial T}{\partial U_i} = 0 \tag{44}$$

The last term of (39) can be simply computed using (41):

$$\frac{\partial V}{\partial U_i} = K_{ij} U_i \tag{45}$$

The equations of motion (39) hence can be written as:

$$M_{ij} a_j + K_{ij} U_i = Q_i \tag{46}$$

4.3 Computation of the stiffness matrix K

The stiffness matrix can be computed from expression (45). This requires that the potential energy is expressed as a function of the degrees of freedom of the system.

The spacial derivatives of the degrees of freedom can also be expressed using the Lagrangian interpolation functions.

$$\frac{\partial w(x)}{\partial x} = \frac{\partial \mathrm{N_j(x)}}{\partial \mathrm{x}} \mathrm{w_j} \tag{47}$$

$$\frac{\partial^2 w(x)}{\partial x^2} = \frac{\partial^2 \mathrm{N_j(x)}}{\partial \mathrm{x}^2} \mathrm{w_j} \tag{48}$$

$$\frac{\partial \alpha(x)}{\partial x} = \frac{\partial \mathrm{N_j(x)}}{\partial \mathrm{x}} \alpha_\mathrm{j} \tag{49}$$

The strain expressions in (25) and (31) can be now rewritten using the interpolation functions:

$$\gamma = \frac{(2\mathrm{h}+\mathrm{h_0})}{\mathrm{h_0}} N_j \alpha_j + \frac{(2\mathrm{h}+\mathrm{h_0})}{\mathrm{h_0}} \frac{\partial \mathrm{N_j}}{\partial \mathrm{x}} \mathrm{w_j} \tag{50}$$

$$\left(\frac{\partial u_O}{\partial x}\right)^2 = \left[\frac{(2\mathrm{h}+\mathrm{h_0})}{2} \frac{\partial \mathrm{N_j}}{\partial \mathrm{x}} \alpha_\mathrm{j} + \frac{h}{2} \frac{\partial^2 \mathrm{N_j}}{\partial \mathrm{x}^2} \mathrm{w_j}\right]^2 \tag{51}$$

The potential energy expression (32) hence becomes:

$$V = \int_{-L/2}^{L/2} E\frac{bh^3}{12}\left(\frac{\partial^2 N_j}{\partial x^2} w_j\right)^2 dx + \frac{1}{2}\int_{-L/2}^{L/2} E_0\frac{bh_0{}^3}{12}\left(\frac{\partial^2 N_j}{\partial x^2} w_j\right)^2 dx + \int_{-L/2}^{L/2} Ebh\left[\frac{(2h+h_0)}{2}\frac{\partial N_j}{\partial x}\alpha_j + \frac{h}{2}\frac{\partial^2 N_j}{\partial x^2} w_j\right]^2 dx + \frac{1}{2}\int_{-L/2}^{L/2} h_0 bG_0\left(\frac{(2h+h_0)}{h_0} N_j\alpha_j + \frac{(2h+h_0)}{h_0}\frac{\partial N_j}{\partial x} w_j\right)^2 dx \quad (52)$$

The derivative of V for the degree of freedom w_i is:

$$\frac{\partial V}{\partial w_i} = E\frac{bh^3}{6}\int_{-L/2}^{L/2}\frac{\partial^2 N_j}{\partial x^2}\frac{\partial^2 N_i}{\partial x^2} w_j\, dx + E_0\frac{bh_0{}^3}{12}\int_{-L/2}^{L/2}\frac{\partial^2 N_j}{\partial x^2}\frac{\partial^2 N_i}{\partial x^2} w_j\, dx + Ebh\int_{-L/2}^{L/2}\left(\frac{(2h+h_0)}{2}\frac{\partial N_j}{\partial x}\alpha_j + \frac{h}{2}\frac{\partial^2 N_j}{\partial x^2} w_j\right) h\frac{\partial^2 N_i}{\partial x^2} dx + h_0 bG_0\int_{-L/2}^{L/2}\left(\frac{(2h+h_0)}{h_0} N_j\alpha_j + \frac{(2h+h_0)}{h_0}\frac{\partial N_j}{\partial x} w_j\right)\frac{(2h+h_0)}{h_0}\frac{\partial N_i}{\partial x} dx \quad (53)$$

Rearranging the terms yields:

$$\frac{\partial V}{\partial w_i} = \left(\frac{2Ebh^3 + E_0 bh_0{}^3}{12}\right)\left(\int_{-L/2}^{L/2}\frac{\partial^2 N_j}{\partial x^2}\frac{\partial^2 N_i}{\partial x^2} dx\right) w_j + \frac{Ebh^3}{2}\left(\int_{-L/2}^{L/2}\frac{\partial^2 N_j}{\partial x^2}\frac{\partial^2 N_i}{\partial x^2} dx\right) w_j + h_0 bG_0\left(\frac{(2h+h_0)}{h_0}\right)^2\left(\int_{-L/2}^{L/2}\frac{\partial N_j}{\partial x}\frac{\partial N_i}{\partial x} dx\right) w_j + Ebh^2\frac{(2h+h_0)}{2}\left(\int_{-L/2}^{L/2}\frac{\partial N_j}{\partial x}\frac{\partial^2 N_i}{\partial x^2} dx\right)\alpha_j + h_0 bG_0\left(\frac{(2h+h_0)}{h_0}\right)^2\left(\int_{-L/2}^{L/2} N_j\frac{\partial N_i}{\partial x} dx\right)\alpha_j \quad (54)$$

The derivative of V for the degree of freedom α_i:

$$\frac{\partial V}{\partial \alpha_i} = 2Ebh\int_{-L/2}^{L/2}\left(\frac{(2h+h_0)}{2}\frac{\partial N_j}{\partial x}\alpha_j + \frac{h}{2}\frac{\partial^2 N_j}{\partial x^2} w_j\right)\frac{(2h+h_0)}{2}\frac{\partial N_i}{\partial x} dx + \frac{h_0 bG_0}{2}\int_{-L/2}^{L/2} 2\left(\frac{(2h+h_0)}{h_0} N_j\alpha_j + \frac{(2h+h_0)}{h_0}\frac{\partial N_j}{\partial x} w_j\right)\frac{(2h+h_0)}{h_0} N_i dx \quad (55)$$

Rearranging the terms yields:

$$\frac{\partial V}{\partial \alpha_i} = Ebh^2 \frac{(2h+h_0)}{2}\left(\int_{-L/2}^{L/2} \frac{\partial^2 N_j}{\partial x^2}\frac{\partial N_i}{\partial x}dx\right) w_j + h_0 bG_0 \left(\frac{(2h+h_0)}{h_0}\right)^2 \left(\int_{-L/2}^{L/2} \frac{\partial N_j}{\partial x} N_i dx\right) w_j + \frac{Ebh(2h+h_0)^2}{2}\left(\int_{-L/2}^{L/2} \frac{\partial N_j}{\partial x}\frac{\partial N_i}{\partial x}dx\right)\alpha_j + h_0 bG_0 \left(\frac{(2h+h_0)}{h_0}\right)^2 \left(\int_{-L/2}^{L/2} N_j N_i dx\right)\alpha_j \quad (56)$$

The sub matrices of the stiffness matrix are hence:

$$[K] = \begin{bmatrix} K_{ij}^{11} & K_{ij}^{12} \\ K_{ij}^{21} & K_{ij}^{22} \end{bmatrix} \quad (57)$$

With:

$$K_{ij}^{11} = \left(\frac{2Ebh^3 + E_0 bh_0{}^3}{12}\right)\left(\int_{-L/2}^{L/2} \frac{\partial^2 N_j}{\partial x^2}\frac{\partial^2 N_i}{\partial x^2}dx\right) + \frac{Ebh^3}{2}\left(\int_{-L/2}^{L/2} \frac{\partial^2 N_j}{\partial x^2}\frac{\partial^2 N_i}{\partial x^2}dx\right) + h_0 bG_0 \left(\frac{(2h+h_0)}{h_0}\right)^2 \left(\int_{-L/2}^{L/2} \frac{\partial N_j}{\partial x}\frac{\partial N_i}{\partial x}dx\right)$$

$$K_{ij}^{12} = Ebh^2 \frac{(2h+h_0)}{2}\left(\int_{-L/2}^{L/2} \frac{\partial N_j}{\partial x}\frac{\partial^2 N_i}{\partial x^2}dx\right) + h_0 bG_0 \left(\frac{(2h+h_0)}{h_0}\right)^2 \left(\int_{-L/2}^{L/2} N_j \frac{\partial N_i}{\partial x}dx\right)$$

$$K_{ij}^{21} = Ebh^2 \frac{(2h+h_0)}{2}\left(\int_{-L/2}^{L/2} \frac{\partial^2 N_j}{\partial x^2}\frac{\partial N_i}{\partial x}dx\right) + h_0 bG_0 \left(\frac{(2h+h_0)}{h_0}\right)^2 \left(\int_{-L/2}^{L/2} \frac{\partial N_j}{\partial x} N_i dx\right)$$

$$K_{ij}^{22} = \frac{Ebh(2h + h_0)^2}{2}\left(\int_{-L/2}^{L/2} \frac{\partial N_j}{\partial x}\frac{\partial N_i}{\partial x}dx\right) + h_0 bG_0\left(\frac{(2h + h_0)}{h_0}\right)^2\left(\int_{-L/2}^{L/2} N_j N_i dx\right)$$

It can be noticed that $K_{ij}^{12} = K_{ji}^{21}$ in the global stiffness matrix and hence the stiffness matrix is symmetric. However, locally, in the submatrices (57), K_{ij}^{12} can be different from K_{ji}^{21}.

4.4 Computation of the Mass matrix M

The mass matrix can be computed from expression (42). The kinetic energy is expressed already directly as a function of the degrees of freedom of the system (33).

$$\mathrm{T} = \frac{1}{2}\int_{-\mathrm{L}/2}^{\mathrm{L}/2}(\rho A + \rho_0 A_0)\left(\frac{\partial w}{\partial \mathrm{t}}\right)^2 d\mathrm{x} + \frac{1}{2}\int_{-\mathrm{L}/2}^{\mathrm{L}/2}(\rho I + \rho_0 I_0)\left(\frac{\partial \alpha}{\partial \mathrm{t}}\right)^2 d\mathrm{x} \quad (33)$$

The time derivatives of the degrees of freedom can be expressed using the Lagrangian interpolation functions.

$$\frac{\partial w(x,t)}{\partial t} = \mathrm{N_j(x)}\frac{\partial \mathrm{w_j}}{\partial \mathrm{t}} = \mathrm{N_j(x)v_j} \quad (58)$$

$$\frac{\partial \alpha(x,t)}{\partial t} = \mathrm{N_j(x)}\frac{\partial \alpha}{\partial \mathrm{t}} = \mathrm{N_j(x)}\omega_\mathrm{j} \quad (59)$$

(33) can now be rewritten as a function of the Lagrange interpolation functions and the velocity v and circular velocity ω.

$$\mathrm{T} = \frac{1}{2}\int_{-\mathrm{L}/2}^{\mathrm{L}/2}(\rho_0 A_0 + \rho A)(N_j \mathrm{v_j})^2 d\mathrm{x} + \frac{1}{2}\int_{-\mathrm{L}/2}^{\mathrm{L}/2}(\rho_0 I_0 + \rho I)(N_j \omega_\mathrm{j})^2 d\mathrm{x} \quad (60)$$

The time derivative of the derivative of V for the degree of freedom v_i:

$$\frac{\partial \mathrm{T}}{\partial \mathrm{v_i}} = (\rho_0 A_0 + \rho A)\left(\int_{-\mathrm{L}/2}^{\mathrm{L}/2} \mathrm{N_j} N_i d\mathrm{x}\right)\mathrm{v_j} \quad (61)$$

$$\frac{\mathrm{d}\left(\frac{\partial \mathrm{T}}{\partial \mathrm{v_i}}\right)}{\mathrm{dt}} = (\rho_0 A_0 + \rho A)\left(\int_{-\mathrm{L}/2}^{\mathrm{L}/2} \mathrm{N_j} N_i d\mathrm{x}\right)\frac{\partial^2 \mathrm{w_j}}{\partial \mathrm{t}^2} \quad (62)$$

The time derivative of the derivative of T for the degree of freedom ω_i:

$$\frac{\partial \mathrm{T}}{\partial \omega_\mathrm{i}} = (\rho_0 I_0 + \rho I)\left(\int_{-\mathrm{L}/2}^{\mathrm{L}/2} \mathrm{N_j} N_i d\mathrm{x}\right)\omega_\mathrm{j} \quad (63)$$

$$\frac{\mathrm{d}\left(\frac{\partial \mathrm{T}}{\partial \omega_\mathrm{i}}\right)}{\mathrm{dt}} = (\rho_0 I_0 + \rho I)\left(\int_{-\mathrm{L}/2}^{\mathrm{L}/2} \mathrm{N_j} N_i d\mathrm{x}\right)\frac{\partial^2 \alpha_\mathrm{j}}{\partial \mathrm{t}^2} \quad (64)$$

The sub matrices of the mass matrix are hence:

$$[M] = \begin{bmatrix} \mathrm{M}_{\mathrm{ij}}^{11} & 0 \\ 0 & \mathrm{M}_{\mathrm{ij}}^{22} \end{bmatrix} \tag{65}$$

With:

$$\mathrm{M}_{\mathrm{ij}}^{11} = (\rho_0 A_0 + \rho A)\left(\int_{-\mathrm{L}/2}^{\mathrm{L}/2} \mathrm{N_j} N_i d\mathrm{x}\right)$$

$$\mathrm{M}_{\mathrm{ij}}^{22} = (\rho_0 I_0 + \rho I)\left(\int_{-\mathrm{L}/2}^{\mathrm{L}/2} \mathrm{N_j} N_i d\mathrm{x}\right)$$

4.5 Stiffness and Mass matrix in local coordinates

The transformation from (x,y) coordinates to local (ξ, η) coordinates is based on the discrete model of the central line of the sandwich beam:

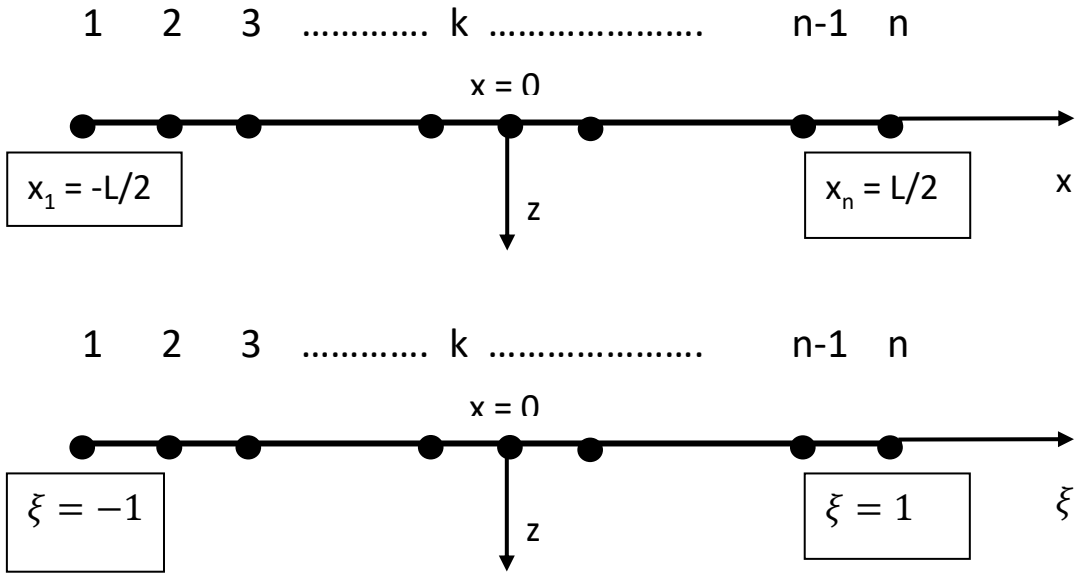

Figure 4.5.1. Discrete numerical model in x and local coordinates ξ

The central line of the laminated beam is divided into a regular grid of n equidistant nodal point. The x axis has its origin in the middle of the beam. The value of ξ in node 1 is –1. The value of ξ in node n is 1. The value of the degrees of freedom $w(\xi)$ and $\alpha(\xi)$ in an arbitrary point ξ of the central line are expressed as a summation of interpolation functions multiplied with the value of the degrees of freedom in the nodal points. High polynomial Lagrange functions are proposed as interpolation functions.

The Lagrangian interpolation function N associated to node k is in x- coordinates:

$$N_k = \frac{(x-x_1)(x-x_2)\ldots(x-x_{k-1})(x-x_{k+1})\ldots(x-x_n)}{(x_k-x_1)(x_k-x_2)\ldots(x_k-x_{k-1})(x_k-x_{k+1})\ldots(x_k-x_n)} \tag{66}$$

The Lagrangian interpolation function N associated to node k is in ξ coordinates:

$$N_k = \frac{(\xi-\xi_1)(\xi-\xi_2)\ldots(\xi-\xi_{k-1})(\xi-\xi_{k+1})\ldots(\xi-\xi_n)}{(\xi_k-\xi_1)(\xi_k-\xi_2)\ldots(\xi_k-\xi_{k-1})(\xi_k-\xi_{k+1})\ldots(\xi_k-\xi_n)} \tag{67}$$

It can be verified that the function N_k equals to 1 in node k and equals to zero in all other nodes.

4.6 Discrete dynamic equations of motion

In the case that external shear forces and couples are acting in the nodal points of the numerical model, the discrete dynamic equations of motion become (double dot means second time derivative):

$$[Q] = [M]\{\ddot{U}\} + [K]\{U\} \tag{68}$$

$$[K] = \begin{bmatrix} K_{11}^{11} & K_{12}^{12} & \cdots & K_{1n-1}^{11} & K_{1n}^{12} \\ K_{21}^{21} & K_{22}^{22} & \cdots & K_{2n-1}^{21} & K_{2n}^{22} \\ \vdots & \vdots & \ddots & \vdots & \vdots \\ K_{n-11}^{11} & K_{n-12}^{12} & \cdots & K_{n-1n-1}^{11} & K_{n-1n}^{12} \\ K_{n1}^{21} & K_{n2}^{22} & \cdots & K_{nn-1}^{21} & K_{nn}^{22} \end{bmatrix}$$

$$[M] = \begin{bmatrix} M_{11}^{11} & 0 & . & . & M_{1n-1}^{11} & 0 \\ 0 & M_{22}^{22} & . & . & 0 & M_{2n}^{22} \\ . & . & . & . & . & . \\ . & . & . & . & . & . \\ . & . & . & . & . & . \\ M_{n-11}^{11} & 0 & . & . & M_{n-1n-1}^{11} & 0 \\ 0 & M_{n2}^{22} & . & . & 0 & M_{nn}^{22} \end{bmatrix}$$

$$\{Q\} = \begin{Bmatrix} Q_1 \\ M_1 \\ \vdots \\ . \\ Q_n \\ M_n \end{Bmatrix}$$

$$\{U\} = \begin{Bmatrix} w_1 \\ \alpha_1 \\ \vdots \\ . \\ w_n \\ \alpha_n \end{Bmatrix}$$

$$\{\ddot{U}\} = \begin{Bmatrix} \ddot{w}_1 \\ \ddot{\alpha}_1 \\ \vdots \\ . \\ \ddot{w}_n \\ \ddot{\alpha}_n \end{Bmatrix}$$

4.7 Section forces

The solution of the set of equations (68) yields the value of the degrees of freedom in each node of the numerical model.

With the obtained values of these d.o.f, the section forces in the nodes i can be computed by post processing:

$$(M_1)_i = (M_2)_i = \frac{Ebh^3}{12}\left(\frac{\partial^2 w}{\partial x^2}\right)_i \qquad i = 1, 2, \dots n \tag{69}$$

$$(M_{inter})_i = \frac{E_0 b h_0^3}{12}\left(\frac{\partial^2 w}{\partial x^2}\right)_i \qquad i = 1, 2, \dots n \tag{70}$$

$$(N)_i = Ebh\left[\frac{(2h+h_0)}{2}\left(\frac{\partial \alpha}{\partial x}\right)_i + \frac{h}{2}\left(\frac{\partial^2 w}{\partial x^2}\right)_i\right] \qquad i = 1, 2, \dots n \tag{71}$$

$$(M_0)_i = (h + h_0)(N)_i \qquad i = 1, 2, \dots n \tag{72}$$

The total bending moment in each node i of the numerical model is the summation of the contributions of all the layers:

$$M = (M_0)_i + (M_{inter})_i + (M_1)_i + (M_2)_i \qquad i = 1, 2, \dots n \tag{73}$$

5 Identification of the transverse shear modulus

5.1 The storage part of the transverse shear modulus G'

5.1.1 Introduction

For the identification of the transverse shear modulus of the polymer interlayer of the laminated glass beam, it is assumed that the isotropic elastic properties of the glass layers are known.

Young's modulus of Glass = 7. E+10 N/m2

Poisson's ratio of Glass = 0.23

Shear modulus of Glass = 2.85E+10 N/m2

It is also assumed that the Poisson's ratio of the polymer interlayer is given. For PVB, the value of Poisson's ratio v = 0.45. Assuming that the polymer material is also isotropic, the Young's modulus E_0 can be computed from the transverse shear modulus G_0:

$$E_0 = 2G_0(1+v) \tag{74}$$

The transverse shear modulus G_0 of the polymer interlayer is hence the only unknown value. In the following paragraphs, it will be described how the value of G_0 can be estimated from the measured first natural frequency of a freely suspended laminated glass beam.

5.1.2 Starting value for the transverse shear modulus

The geometrical sizes and the mass of the test beam are assumed to be known. The eigenvalue of the test beam will fall in an interval bounded by two extreme values. The maximal eigenvalue is associated with a monolithic glass beam and the minimal eigenvalue is associated with the beam with independent bending of the two glass layers.

The bending stiffness of a monolithic beam E = E_{Glass} is:

$$(EI)_{monolith} = E\frac{b(2h+h_0)^3}{12} \tag{75}$$

The bending stiffness for two separate layers can be computed as:

$$(EI)_{two\ separate\ glass\ beams} = Eb\frac{h^3}{6} \tag{76}$$

The eigenvalue of a freely suspended beam with equivalent stiffness value EI (considered as an Euler Bernoulli beam) can be computed:

$$\lambda = \frac{501(\mathrm{EI})_{\mathrm{Equivalent}}}{\mathrm{L}^3(\mathrm{Beam\ Mass})} \tag{77}$$

A starting value for the shear modulus G_0 can now be computed with a linear interpolation formula:

$$\mathrm{G_{Start}} = \mathrm{G_{Glass}}\frac{\lambda-\lambda_{\mathrm{Separate\ Beams}}}{\lambda_{\mathrm{Monolith}}-\lambda_{\mathrm{Separate\ Beams}}} \tag{78}$$

In which λ is the measured eigenvalue.

5.1.3 Improving the shear Modulus by subsequent bisections

With the starting value G_{Start}, a new first eigenvalue of the glass beam can be computed with the numerical model. The new first eigenvalue can be situated in the interval with the extreme values.

If the new eigenvalue is bigger than the measured eigenvalue, the value of the shear modulus $G = G_0$ is dived by 2 and a new eigenvalue is again computed. This is continued till the computed eigenvalue is lower than the measured value.

In the opposite case, the shear modulus G is multiplied with 2 and this is repeated till the computed eigenvalue is bigger than the measured value.

The value of the shear modulus G for the computed eigenvalue λ_{Min} that is just lower than the measured value is taken as G_{min}, the one that for a just higher computed eigenvalue λ_{Max} is taken as G_{max}.

At the end of this bisection sequence, an improved value for the shear modulus can be computed by interpolation.

$$G = G_{Min} + (G_{Max} - G_{Min}) \frac{\lambda - \lambda_{Min}}{\lambda_{Max} - \lambda_{Min}} \tag{79}$$

5.1.4 Further improvement of the shear modulus by sensitivity computations

The eigenvalue problem for the first eigenvalue λ_1 and the first eigenvector can be expressed as a function of the Stiffness and Mass Matrix.

$$\left(\begin{bmatrix} K_{ij}^{11} & K_{ij}^{12} \\ K_{ij}^{21} & K_{ij}^{22} \end{bmatrix} - \lambda_1 \begin{bmatrix} M_{ij}^{11} & 0 \\ 0 & M_{ij}^{22} \end{bmatrix} \right) \{\emptyset_1\} = \{0\} \tag{80}$$

The following coefficients can be introduced (neglecting the bending contribution of E_0):

$$C1 = \frac{2bh^3}{3} \tag{81}$$

$$C2 = h_0 b \left(\frac{(2h + h_0)}{h_0} \right)^2 \tag{82}$$

$$C3 = bh^2 \frac{(2h + h_0)}{2} \tag{83}$$

$$C4 = \frac{bh(2h + h_0)^2}{2} \tag{84}$$

The following matrices can be introduced:

$$A_{ij} = \int_{-L/2}^{L/2} \frac{\partial^2 N_j}{\partial x^2} \frac{\partial^2 N_i}{\partial x^2} dx \quad B_{ij} = \int_{-L/2}^{L/2} \frac{\partial N_j}{\partial x} \frac{\partial^2 N_i}{\partial x^2} dx \quad C_{ij} = \int_{-L/2}^{L/2} \frac{\partial N_j}{\partial x} \frac{\partial N_i}{\partial x} dx$$

$$D_{ij} = \int_{-L/2}^{L/2} \frac{\partial N_j}{\partial x} N_i dx \quad E_{ij} = \int_{-L/2}^{L/2} N_j N_i dx \quad F_{ij} = \int_{-L/2}^{L/2} \frac{\partial^2 N_j}{\partial x^2} \frac{\partial N_i}{\partial x} dx$$

$$G_{ij} = \int_{-L/2}^{L/2} N_j \frac{\partial N_i}{\partial x} dx \tag{85}$$

The terms occurring in (57) can now be written shortly as:

$$\mathrm{K}_{\mathrm{ij}}^{11} = E.C1\left[A_{ij}\right] + G.C2\left[\mathrm{C}_{\mathrm{ij}}\right]$$

$$\mathrm{K}_{\mathrm{ij}}^{12} = \mathrm{E}.C3\left[B_{ij}\right] + G.C2\left[\mathrm{D}_{\mathrm{ij}}\right]$$

$$\mathrm{K}_{\mathrm{ij}}^{21} = \mathrm{E}.C3\left[F_{ij}\right] + G.C2\left[\mathrm{G}_{\mathrm{ij}}\right]$$

$$\mathrm{K}_{\mathrm{ij}}^{22} = E.C4\left[C_{ij}\right] + G.C2\left[\mathrm{E}_{\mathrm{ij}}\right]$$

The stiffness matrix can be written as:

$$\begin{bmatrix} \mathrm{K}_{\mathrm{ij}}^{11} & \mathrm{K}_{\mathrm{ij}}^{12} \\ \mathrm{K}_{\mathrm{ij}}^{21} & \mathrm{K}_{\mathrm{ij}}^{22} \end{bmatrix} = \mathrm{G}.\begin{bmatrix} \mathrm{C2C}_{\mathrm{ij}} & \mathrm{C2D}_{\mathrm{ij}} \\ \mathrm{C2G}_{\mathrm{ij}} & \mathrm{C2E}_{\mathrm{ij}} \end{bmatrix} + \mathrm{E}.\begin{bmatrix} \mathrm{C1A}_{\mathrm{ij}} & \mathrm{C3B}_{\mathrm{ij}} \\ \mathrm{C3F}_{\mathrm{ij}} & \mathrm{C4C}_{\mathrm{ij}} \end{bmatrix} \tag{86}$$

Shortly:

$$[\mathrm{K}] = \mathrm{G}.[\mathrm{X}] + \mathrm{E}.[\mathrm{Y}] \tag{87}$$

Pre-multiplying (88) with the first eigenvector $\{\emptyset_1\}^\tau$ and considering the normalisation $\{\emptyset_1\}^\tau[\mathrm{M}]\{\emptyset_1\} = [\mathrm{I}]$ gives:

$$\{\emptyset_1\}^\tau(G[\mathrm{X}] + \mathrm{E}.[\mathrm{Y}])\{\emptyset_1\} = \lambda_1 \tag{88}$$

And finally:

$$G = \frac{\lambda_1 - \{\emptyset_1\}^\tau E.[Y]\{\emptyset_1\}}{\{\emptyset_1\}^\tau[X]\{\emptyset_1\}} \tag{89}$$

It can be seen in (89) that the knowledge of the first experimental eigenvalue and the eigenvector computed with starting values for G allows to estimate an updated value of G. The refined value of G can be used to re-compute the first eigenvector and hence the final value of G can be obtained by iteration using (89).

5.1.5 Sensitivity of the eigenvalue for the shear modulus G

Expression (89) can be used the compute the sensitivity of the eigenvalue for variations of the shear modulus G.

$$\frac{\partial \lambda}{\partial G} = \{\emptyset_1\}^\tau [X] \{\emptyset_1\} \tag{90}$$

If the value of the derivative in (90) is very low, this means that variations of G nearly don't influence the value of the eigenvalue λ, hence in that case identification of G will be very difficult.

The sensitivity can be approximated by finite variations: $\frac{\partial \lambda}{\partial G} = \frac{\Delta \lambda}{\Delta G}$

The relative sensitivity is: $$RelSens = \frac{G \Delta \lambda}{\lambda \Delta G} \tag{91}$$

A variation of 1 Hz causes a relative variation $\frac{\Delta \lambda}{\lambda}$ of the eigenvalue:

$$\lambda_{Rel} = \frac{\Delta \lambda}{\lambda} = \frac{((F_{Measured} + 1Hz) 2\pi)^2 - \lambda}{\lambda} \tag{92}$$

The percentage uncertainty for the G-Modulus for a 1 Hz variation is hence:

$$\frac{\Delta G}{G} . 100 = \frac{\lambda_{Rel}}{RelSens} 100 \tag{93}$$

The accuracy of a measurement of the resonance frequency using the impulse excitation method is 0.1%. So alternatively, it can be computed how much an error of 0.1% on the resonance frequency influences the uncertainty of the obtained value for the transverse shear storage modulus G.

An accuracy of 0.1% on the resonance frequency yields an accuracy of 0.2 % on the eigenvalue. The % uncertainty on the obtained G is hence:

$$\%\ Uncertainty\ on\ G = \frac{0.02}{RelSens} 100 \tag{94}$$

5.1.6 Example of identification of G

The test beam is a laminated glass beam with a very thin PVB interlayer:

Length Beam	:	.25 m
Width Beam	:	2.93300E-02 m
Thick Glass layer	:	3.85000E-03 m
Thick Poly layer	:	3.90000E-04 m
Specific Mass Glass:		2480.0 kg/m3
Specific Mass Poly :		1100.0 kg/m3
Beam Mass	:	.14317 kg
E-modulus Glass	:	7.00000E+10 N/m2

The measured first Frequency is 698.00 Hz

The next paragraphs illustrate the starting procedure, the bisections, the interpolation and finally the iterations on the G value.

5.1.6.1 Starting value

Measured first Eigenvalue	:	1.92340E+07
Minimal Eigenvalue (independent layers)	:	4.37336E+06
Maximal Eigenvalue (monolith)	:	2.02885E+07

EI-Min	:	19.527 Nm2
EI-Max:		90.589 Nm2

Obtained starting value for the Shear modulus of the PVB layer :

G_{Start} = 6.53E+10 N/m2

With a value 0.45 for Poisson's ratio, the Young's Modulus of the PVB layer E_0 becomes: 1.89551E+11 N/m2

5.1.6.2 Bisections

The first interval for the eigenvalues is bounded by the monolith and the separate beams boundaries. Next subsequent bisections isolate the measured eigenvalue between more and more sharp boundaries

Iteration number	Transverse shear G N/m2	Computed eigenvalue	Computed natural frequency Hz	Measured natural frequency Hz
1	6.53E+010	1.99E+007	711.75	698
2	3.26E+010	1.99E+007	711.65	698
3	1.63E+010	1.99E+007	711.54	698
4	8.17E+009	1.99E+007	711.35	698
5	4.08E+009	1.99E+007	711.00	698
6	2.04E+009	1.99E+007	710.31	698
7	1.02E+009	1.98E+007	708.95	698
8	5.10E+008	1.96E+007	706.27	698
9	2.55E+008	1.94E+007	701.09	698
10	1.28E+008	1.88E+007	691.32	698

Table 5.1.6.2.1. G-modulus during subsequent bisections

It can be observed that after the 10^{th} bisection the value of the computed natural frequency became lower than the measured value. It is also observed that at the start the value of the G modulus hardly influences the eigenvalue. This means the eigenvalue i not very sensitive for variations of G.

5.1.6.3 Interpolated value at the end of the bisections

At the end of the bisection the situation is as follows:

G_{Min} = 1.28E+008

G_{Max} = 2.55E+008

FREQ Min = 691.32 Hz

FREQ Max = 701.09 Hz

With these values, an interpolated value for G can be computed using (79):

$$G_{Interpolated} = 2.14E+008 \text{ N/m2}$$

5.1.6.4 Direct iteration on the eigenvalue expression

G_{Final} = 1.95E+08 N/m2

FREQ Numerical = 697.99 Hz

FREQ Measured = 698.00 Hz

The sensitivity of lambda for G is $\frac{\partial \lambda}{\partial G}$ = 3.73E-003

The percentage uncertainty for G for a 1 Hz Measurement error = 7.58%

This shows that a very small error on the measured frequency of 1 Hz already causes a large percentage uncertainty of 7.58%. This is due to the low sensitivity value of the eigenvalue for variations of G.

5.1.6.5 Conclusion

Even for very lows sensitivities, the combination of bisections, interpolation and direct iteration allows estimating the transverse shear modulus of the PVB layer. However, a small variation on the measured frequency immediately causes a large uncertainty on the final result for G. The source of variation on the measured frequency must be combined with the uncertainty of the correctness of the numerical model versus the real test sample. Non-correct physical input values like the Young's modulus of glass, the density of the used materials and the geometrical data like length, width and thicknesses of the layers cause differences between the real physical model and the numerical model.

5.1.7 Influence of the G-Modulus on the beam frequency

The natural frequencies computed with the finite element software ABAQUS are used to validate the value of the identified shear modulus. The G-modulus is estimated with the identification procedure.

Case Nr.	$F_{Num.Model}$ [Hz]	G-Modulus Polymer [Pa]	Estimated G-Modulus [Pa]	% error on obtained shear modulus	Sensitivity of eigenvalue
1	1215	2.69E+10	2.46E+10	8.43	1.03E-05
2	1124	2.69E+09	2.57E+09	4.38	7.51E-04
3	958	2.69E+08	2.67E+08	0.73	3.85E-02
4	542	2.69E+07	2.67E+07	0.58	0.27
5	282	2.69E+06	2.64E+09	1.82	0.45
6	225	2.69E+05	2.33E+05	13.51	0.49
7	218	2.69E+04	8.34E+03	131	0.49

Table 5.1.7.1. Identification of the G-Modulus

The identification procedure is capable of estimating nearly all the G-Modulus values correctly. However, the given frequencies are computed hence free of error. It can be seen that the expected % error if the measured frequency is just added 1 Hz is considerable for cases 1, 2, 6 and 7. Only cases 3-5 have reasonable % errors and hence are stable.

As a test, the value of the natural frequency of case 1 (1215 Hz) and 6 (225 Hz) is added and subtracted with 1 Hz.

Case Nr.	$F_{Num.Model}$ [Hz]	G-Modulus Polymer [Pa]	Estimated G-Modulus [Pa]	% Difference for G-Modulus
1 bis	1216	2.69E+10	2.67E+10	+8.45
1 ter	1214	2.69E+10	2.25E+10	-8.4
6 bis	226	2.69E+05	2.61+05	+11.97
6 ter	224	2.69E+07	1.97E+05	-15.53

Table 5.1.7.2. Increased error on the estimated G-Modulus by 1 Hz difference

It is instructive to plot the frequency value of the laminated beam as a function of the G-Modulus (Figure 5.1.7.1). A typical S-shape occurs. The two flat extremes are zones were the frequency doesn't change much with variations of

the G-Modulus. The flat parts are zones of high uncertainty for the obtained storage modulus G, hence not suitable for identification of the G-modulus.

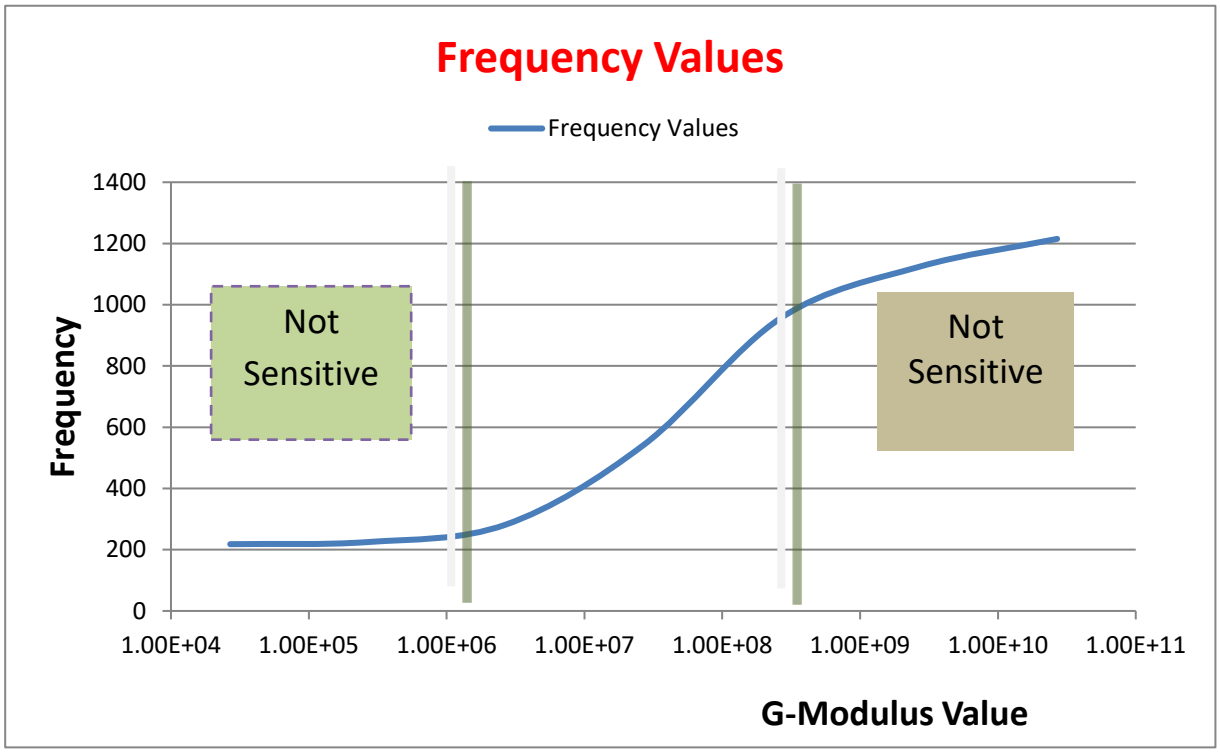

Figure 5.1.7.1. Evolution of the frequency as a function of the G-Modulus value

5.2 The loss part of the Transverse shear modulus G”

5.2.1 Single degree of freedom systems (SDOF)

Very often, linear visco-elastic material behavior is described phenomenological by a simple single degree of freedom SDOF model x(t), consisting of a mass m, a spring k and a dashpot c. The dynamic equilibrium equation for free damped vibrations of this single degree of freedom system is:

$$m\ddot{x}(t) + c\dot{x}(t) + kx(t) = 0 \tag{95}$$

The solution of this equation leads to:

$$x(t) = Xe^{-\xi\omega_0 t}\, sin\omega_d\, t \tag{96}$$

With $\omega_0 = \sqrt{\frac{k}{m}}$ the undamped circular resonance frequency (97)

X the maximal amplitude value

$\omega_d = \omega_0\sqrt{1-\xi^2} \approx \omega_0$: the damped circular resonance frequency

$\xi = \frac{c}{2\sqrt{km}}$: the damping ratio (98)

The response is represented graphically in figure 5.2.1.1

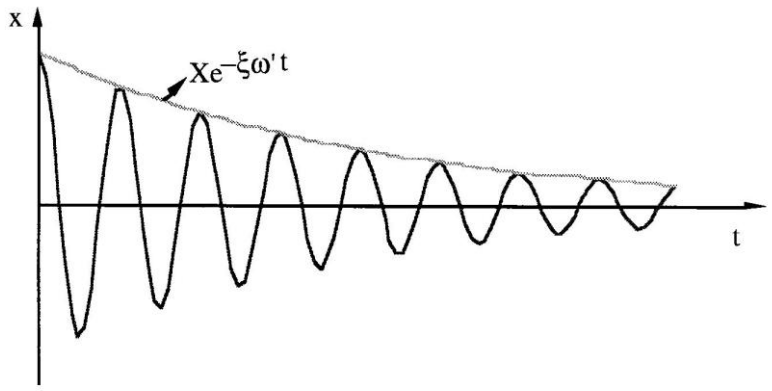

Figure 5.2.1.1 Free damped harmonic vibrations

The damping ratio can be related to the “Specific Damping Capacity” SDC Ψ. For the SDOF-system, one can express the energy quantities (the potential energy P and the damping energy D):

$$P = \frac{1}{2}kX^2 \tag{99}$$

$$D = \pi c \omega_d X^2 \approx \pi c \omega_0 X^2 \tag{100}$$

The "Specific Damping Capacity" SDC Ψ becomes:

$$\Psi = \frac{D}{P} = \frac{\pi c \omega_0 X^2}{\frac{1}{2}kX^2} = \frac{2\pi c \omega_0}{k} \tag{101}$$

Using the expressions in (97) and (98):

$$\Psi = \frac{D}{P} = \frac{2\pi c \omega_0}{k} = \frac{2\pi c}{\sqrt{km}} = 4\pi\xi \tag{102}$$

5.2.2 Multi degree of freedom systems

For a multi degrees of freedom system, the equation becomes:

$$[M]\{\ddot{x}(t)\} + [C]\{\dot{x}(t)\} + [K]\{x(t)\} = 0 \tag{103}$$

In (103) [M], [C] and [K] are the mass, damping and stiffness matrices.

Using the technique of modal decoupling for proportionally damped systems, it is possible to treat a system with n degrees of freedom as n decoupled SDOF-systems. Therefore, the dynamic equilibrium equation is transformed to the basis of modal coordinates:

$$\{x(t)\} = [\phi]\{q(t)\} \tag{104}$$

With {x (t)}: the physical coordinates

{q (t)}: the modal coordinates

$[\phi]$: the matrix formed with the eigenmodes as columns

These modal coordinates {q(t)} can be physically interpreted as the participation factors of the individual modal shapes to the vibration of the structure.

This means that a structure vibrating in one of its eigenmodes can be treated as a SDOF-system in the basis of the modal coordinates, where the single coordinate q (t) represents the amplitude at time t.

The freely damped vibrations of a structure vibrating in eigenmode $\{\phi\}_n$, can thus be written as:

$$x(t) = \{\phi\}_n q_n(t) \tag{105}$$

where, in analogy with the SDOF-system solution (4.1.2):

$$q_n(t) = Q_n e^{-\xi_n \omega_n t} \sin\omega_n t \tag{106}$$

Finally, one obtains the expression:

$$\{x(t)\} = \{\phi\}_n Q_n e^{-\xi_n \omega_n t} \sin\omega_n t \tag{107}$$

where $\{\phi\}_n$: normalized modal shape

ω_n: Circular resonant frequency

ξ_n: Modal damping ratio associated to the modal shape

The analogy between a structure vibrating in one eigenmode (106) and a SDOF-system (96) also allows writing:

$$\xi_n = \frac{D}{4\pi P} \tag{108}$$

5.2.3 Relation of a measured damping ratio with material damping

To find the relation with the loss modulus of a material the dynamic equilibrium equation for a free vibration of a beam made of material with Young's modulus E must be solved for a complex value of E*.

$$E^* I \frac{\partial^4 w(x,t)}{\partial x^4} + \rho A \frac{\partial w(x,t)}{\partial t^2} = 0 \tag{109}$$

(ρ is the density, I is the inertia of the beam and A is the cross section)

The free damped vibrations of the beam vibrating in eigenmode $\{\phi\}$ in pure bending can be written as (separation of a time and space dependent solution):

$$w(x,t) = \{\phi(x)\} q(t) \tag{110}$$

This is a single degree of freedom system with the *q(t)* as the modal coordinate. The pure bending modal shape $\{\phi(x)\}$is the space dependant part.

Substitution of (110) in (109)

$$\frac{E^* I}{\rho A.\phi(x)} \frac{\partial^4 \phi(x)}{\partial x^4} = -\frac{1}{q(t)} \frac{\partial^2 q(t)}{\partial t^2} = \omega^{*2} \tag{111}$$

The equality (111) must be valid for all x and all t and because of the even derivation degrees both parts must be equal to a positive complex constant ω^{*2}

(111) can be written as two separate equations. In the first equation the value of $\Psi$is real because only normal modal shapes are assumed.

$$\frac{\partial^4 \phi(x)}{\partial x^4} - \Omega^4 \phi(x) = 0$$

$$\frac{\partial q^2(t)}{\partial t^2} + \omega^{*2} q(t) = 0 \qquad (112)$$

With: $$\Omega^4 = \frac{\rho A \omega^{*2}}{E^* I} \qquad (113)$$

For an undamped system, $\omega^* = \omega'$and (113) can be rewritten:

$$\omega' = \Omega^2 \sqrt{\frac{EI}{\rho A}} \qquad (114)$$

A proposal for the solution of the time dependent equation is:

$$q(t) = Q(x).e^{i\omega^* t} \qquad (115)$$

The complex number ω* can be expressed as the sum of a real and imaginary part $\omega^* = \omega' + i\omega" = \omega'(1 + i\frac{\omega"}{\omega'})$. If $\frac{\omega"}{\omega'}$is set equal to ξ, the value becomes $\omega^* = \omega'(1 + i\xi)$ and the solution (115) can be written as:

$$q(t) = Q(x).e^{-\xi\omega' t} e^{i\omega' t} \qquad (116)$$

This is the pure bending modal shape q(t) with a circular resonance frequency of ω' and a modal damping ratio ξ. Q(x) is the spatial distribution of the modal shape as solution of the spatial equation.

From (106) can be found that:

$$\omega^* = \Omega^2 \sqrt{\frac{E^* I}{\rho A}} = \Omega^2 \sqrt{\frac{I}{\rho A}} \sqrt{E' + iE"} = \Omega^2 \sqrt{\frac{I}{\rho A}} \sqrt{E'(1 + i\frac{E"}{E'})}$$

$$\omega^* = \Omega^2 \sqrt{\frac{E'I}{\rho A}} \sqrt{1 + itg\delta(E)} = \omega' \sqrt{1 + itg\delta(E)} \qquad (117)$$

Because the tg δ values are small, the complex value ω* can be approximated:

$$\omega^* = \omega'\sqrt{1 + itg\delta(E)} = \omega'(1 + i\frac{tg\delta(E)}{2} + O^2(tg\delta) \approx \omega'(1 + i\frac{tg\delta(E)}{2}).$$

Comparison with $\omega^* = \omega'(1 + i\xi)$ shows that the modal damping ratio $\xi$of the pure bending mode has the double value of the tg δ (E).

$$\xi = \frac{tg\delta(E)}{2} \tag{118}$$

With expression (118), the modal damping ratio and the tangents delta of Young's modulus E can be related to the Specific Damping Capacity (SDC) Ψ.

$$\Psi = \frac{D}{P} = 4\pi.\xi = 2\pi.tg\delta(E) \tag{119}$$

$$tg\delta(E) = \frac{D}{2\pi P} \tag{120}$$

5.2.4 Tangents delta of a sandwich beam

If the vibrating sandwich beam is considered as a homogeneous beam made of a single material with Young's modulus E, the tangents delta of this apparent material is given by expression (120).

For a sandwich beam, the total potential energy (32) has contributions from the glass and PVB layers.

An expression that derives the contributions of every layer (Potential energy of the bending of both glass layers $PE_{GlassBending}$, the potential energy of the normal force N in the glass layers $PE_{GlassNormalForce}$, the potential energy due to bending of the PVB layer $PE_{PVBBending}$and the potential energy due to shearing of the PVB layer PE_{PVB}) to the measured damping ration can be found in [1]:

$$\xi_{Measured} = \frac{1}{2}(\frac{PE_{GlassBending}}{TotalPE} tan\,\delta\,(E)_{Glass} + \frac{PE_{GlassNormalForce}}{TotalPE} tan\,\delta\,(E)_{Glass}$$

$$+ \frac{PE_{PVBBending}}{TotalPE} tan\,\delta\,(E)_{PVB} + \frac{PE_{PVB}}{TotalPE} tan\,\delta\,(G)_{PVB}) \tag{116}$$

For the computation of the tangents delta of the PVB, only the potential energy contribution of the sheared PVB layer has to be taken into account. It is logically assumed that all the dissipated energy originates purely from the shearing behavior of the PVB layer.

$$\xi_{Measured} = \frac{1}{2}(\frac{PE_{PVB}}{TotalPE} tan\,\delta\,(G)_{PVB}) \tag{117}$$

The dissipated energy and the potential energy of the PVB layer must be evaluated and used in expression (115) to obtain the tangents delta of the shear modulus of the PVB.

$$tan\,\delta\,(G)_{PVB} = \frac{Dissipated\ Energy}{2\pi(PE)_{PVB}} = \frac{2\xi_{Measured}}{(PE)_{PVB}/TotalPE} \qquad (118)$$

5.2.5 Example of identification of the tangents delta of G

To validate the correct value of the potential and kinetic energy computed with the numerical model, the following example computes both values

Length Beam	:	0.30000
Width Beam	:	3.02000E-02
Thick skin layer	:	4.94300E-03
Thick Poly layer	:	2.24000E-03
Specific Mass skin:		2475.0
Specific Mass Poly:		1065.0
Beam Mass	:	0.24329
E-modulus skin	:	7.09000E+10
E-modulus Poly	:	4.23100E+08
Measured Frequency:		625.00
Measured damping ratio:		2.1234

The result is:

COMPUTED SANDWICH FREQUENCY:	934.89 Hz
TOTAL POTENTIAL ENERGY:	7.71063E+06
CONTRIBUTION BENDING MOMENT:	1.74185E+06
CONTRIBUTION NORMAL FORCE:	3.58311E+06
CONTRIBUTION SHEAR FORCE:	2.38543E+06
CONTRIBUTION BENDING CORE:	232.02
TOTAL KINETIC ENERGY:	7.71063E+06
CONTRIBUTION MASS:	7.67882E+06
CONTRIBUTION INERTIA:	31806.

It can be observed that the total potential energy is exactly equal to the total kinetic energy (this is Rayleigh's principle).

For a measured damping ratio of 2.1234%, the tangents delta can be computed with (116)

$$tan\,\delta\,(G)_{PVB} = \frac{Dissipated\ Energy}{2\pi(PE)_{PVB}} = \frac{2\xi_{Measured}}{(\frac{PE)_{PVB}}{TotalPE}} = \frac{2x0.02134}{2.3854E{+}06/7.71063} \quad (118)$$

$$tan\,\delta\,(G)_{PVB} = 0.137$$

Ref. [1] Sol, H.; Rahier, H.; Gu, J. Prediction and Measurement of the Damping Ratios of Laminated Polymer Composite Plates. *Materials* **2020**, *13*

5.2.6 Measurement using the impulse excitation Technique

The impulse excitation technique (IET) is a non-destructive material characterization technique to determine the elastic properties. It measures the resonant frequencies to calculate the Young's modules, shear modules, Poisson's ratio and internal friction of predefined shapes like rectangular bars and cylindrical rods. The procedure involves striking the specimen with a small hammer and recording the induced vibration using an accelerometer. The resulting vibration signal, known as the impulse response function (IRF), contains information about the resonance frequency and the damping ratio. Fig 5.2.4.1 illustrates the excitation of a beam, the beam specimen is suspended at its nodal lines (the set of points with zero vibration amplitudes during a bending modal shape), while the excitation and measurement locations are positioned where the vibration amplitude is sufficiently high, typically near the midpoint of the beam.

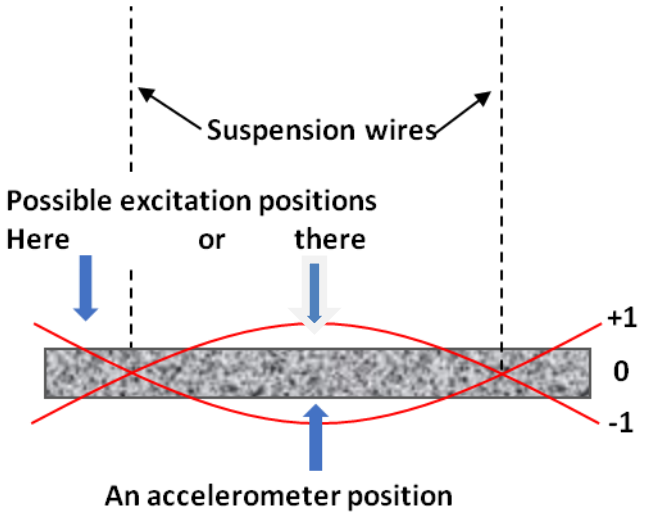

Fig. 5.2.6.1. Excitation position and measurement position for IET tests on test beams

Figures 5.2.6.2 and 5.2.6.3 illustrate the measurement of the resonance frequency using the Resonalyser instrument and the identification of the damping ratio.

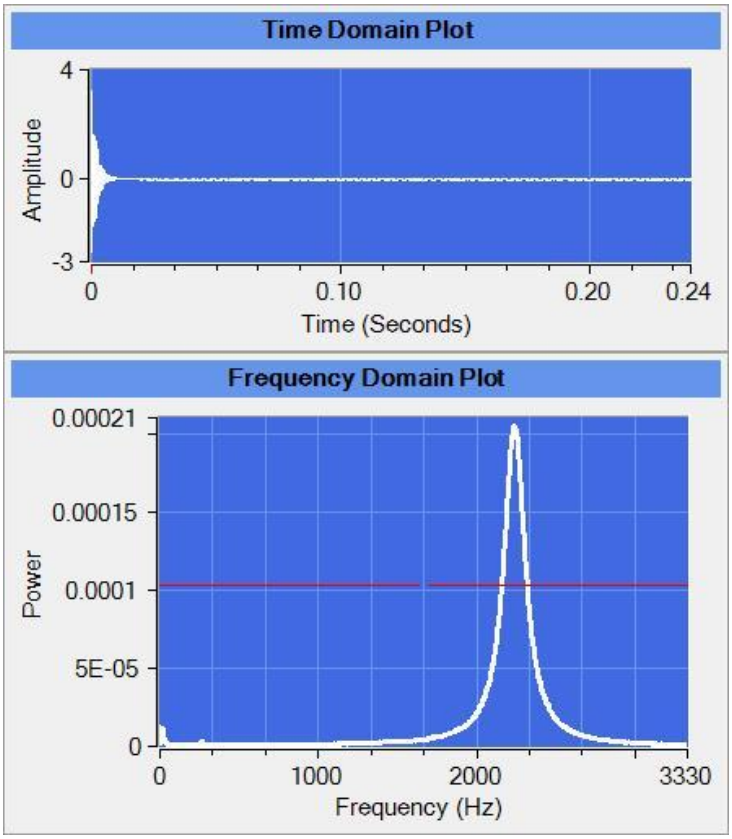

Figure 5.2.6.2. Measurement of the resonance frequency with impulse excitation

Figure 5.2.6.3. Measurement of the damping ratio with impulse excitation

6 Model with variable thickness

The test on the glass sandwich beams have shown that the thickness of the PVB layer and the thickness of the glass layers are important for the final identified value of the transverse shear modulus of the PVB material. The measured glass thickness in the beams and plates in chapter 1 was varying between the values 0.0480 m and 0.0497 m with an average value of 0.0493 m. It was decided to investigate more in detail the thickness of the PVB layer and the glass layers. Therefore the thicknesses are measured with a digital electronic outside micrometer (type Filetta of the company Schut) with 0.001 precision and measurement pressure control (see Figure)

Figure 6.1. Giletta electronic micrometer (Shut)

It was found that the two glass layers of the beams didn't have the same thickness. One layer had a thickness varying between 4.95 and 4.99 with an average value of 4.992 mm; the other layer had a thickness varying between 4.80 and 4.92 with an average thickness of 4.894 mm. Since the mathematical model is symmetric, it was decided to take a constant value of 4.943 mm for both glass layers.

If it is assumed that the glass thickness is constant, but the total thickness is not constant then the consequence will be that the inner PVB layer thickness h_0 is not constant. To take the variation of the thickness of the PVB layer into account, a new numerical model with variable PVB thickness was developed. The model can have a different thickness in every 11 nodal points.

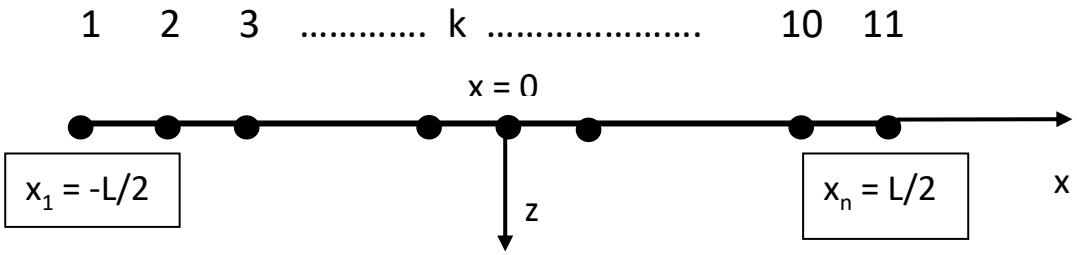

Figure 6.2. Discrete numerical model of the laminate beam with 11 nodes

The Lagrangian interpolation function N associated to node k is in ξ coordinates:

$$N_k = \frac{(\xi-\xi_1)(\xi-\xi_2)\ldots(\xi-\xi_{k-1})(\xi-\xi_{k+1})\ldots(\xi-\xi_n)}{(\xi_k-\xi_1)(\xi_k-\xi_2)\ldots(\xi_k-\xi_{k-1})(\xi_k-\xi_{k+1})\ldots(\xi_k-\xi_n)} \quad (119)$$

It can be verified that the function N_k equals to 1 in node k and equals to zero in all other nodes. This interpolation functions can be used to compute the value of the thickness in the Gauss points of the numerical model:

$$Thick_{Gauss} = \sum_{k=1}^{n} Thick_{Node\ k} \,.\, N_k(\xi_{Gauss}) \quad (120)$$

7 Transverse shear modulus as function of temperature

The IET test can be automatically executed in a climate chamber. The temperature can be programmed between -10°C and + 40°C. The impulse excitation can be performed with a pendulum system.

Figure 7.1. Climate chamber with pendulum excitation

The driving force for an impact is given by solenoids (yellow in figure 7.1)

An example is given for the identification of the transverse shear storage modulus G' and the tangents delta (G) in a temperature interval starting at minus 10°C till plus 40°C (figure 7.2).

The sandwich test beam has the following data:

Length Beam	:	0.30000 m
Width Beam	:	3.02000E-02 m
Thick skin layer	:	4.94300E-03 m
Thick Poly layer	:	2.24000E-03 m
Specific Mass skin:		2475.0 kg/m3
Specific Mass Poly:		1065.0 kg/m3
E-modulus Glass	:	7.09000E+10 Pa

An assumed starting value for the E-modulus of the PVB was taken as 4.00E+08 Pa

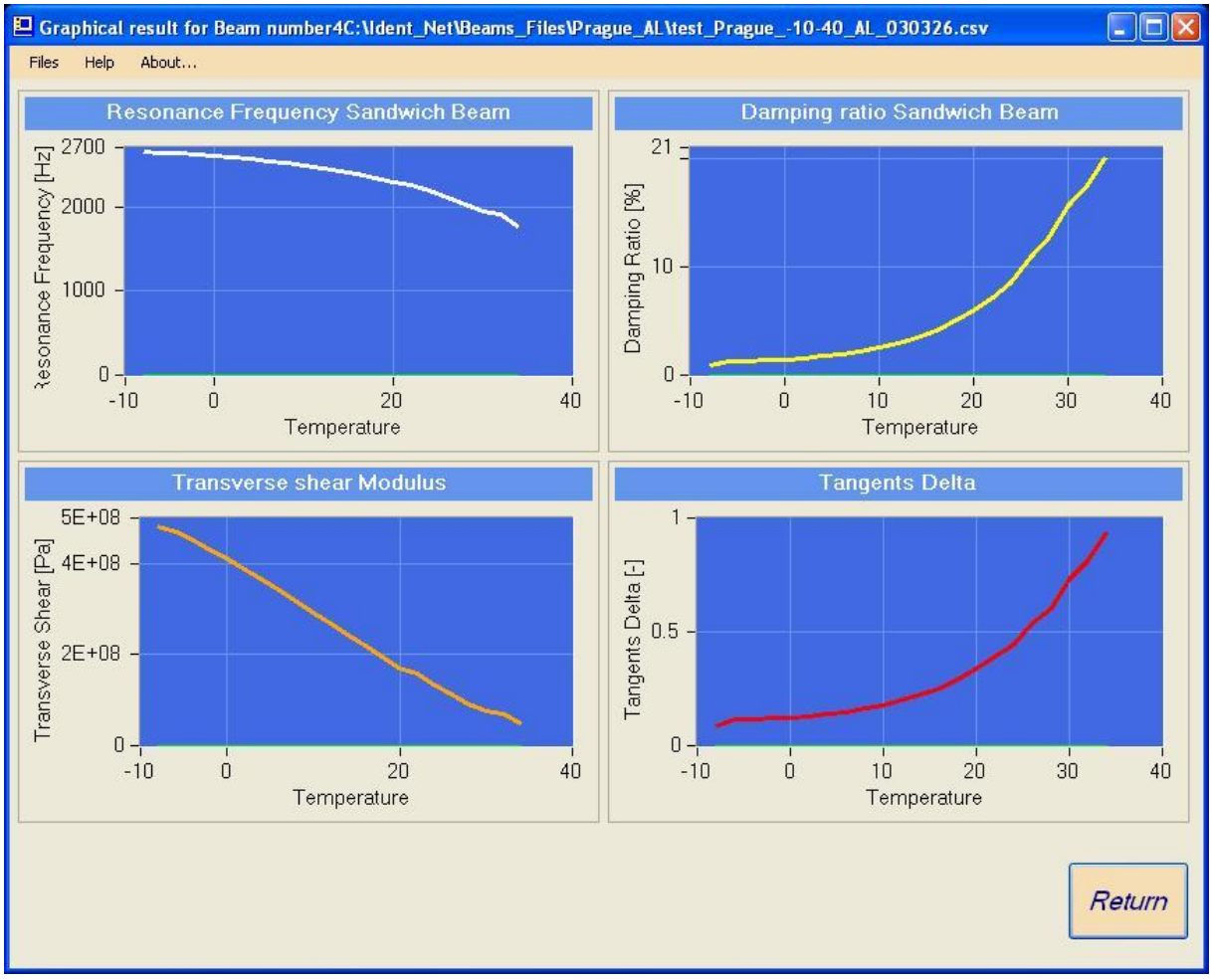

Figure 7.2. The measured resonance frequency and damping ratio (upper graphs) and the identified storage modulus and tangents delta (lower graphs)

It can be seen that the measured resonance frequency and the identified storage modulus decrease with increasing temperature, while the measured damping ratio and the identified tangents delta increase with increasing temperature.

8 Identification of glass properties as a function of temperature

8.1 Introduction

Most models for glass/PVB sandwich samples assume a constant storage Young's modulus of the glass and a neglectable loss modulus in a large temperature range. In this report, it is examined how the storage and loss modulus of glass evolves in a common usage interval with temperatures of -10°C and + 50°C.

8.2 Glass testing by the Impulse excitation technique

The identification of the properties of glass can be automatically executed in a climate chamber. The temperature can be programmed between -10°C and + 50°C. The impulse excitation technique can be performed with a pendulum system.

Figure 8.2.1. Climate chamber with pendulum excitation

A pure glass test plate with sizes 0.2995 m x 0.2995 m x 0.00497 m and a mass of 1.103 kg is freely suspended inside the climate chamber. The measured “Impulse Reponse Function” (IRF) after an impact contains enough information to extract the basic resonance frequency and damping ratio as a function of different temperature steps. The storage modulus and tangents delta of the Young’s modulus, the Poisson’s ratio and the in-plane shear modulus are identified using the Resonalyser procedure. The glass test plate is assumed to be isotropic.

8.3 Test Results on a glass plate

An accelerometer of 0.00035 kg is fixed on the test plate. The measured IRF signal is send to a data acquisition unit of a PC. The Resonanyser software extracts the resonance frequencies (white lines in the figure 8.3.1) and damping ratio (red lines in the figure 8.3.1) of the torsion and breathing modal shapes. The climate chamber starts at a temperature of -10°C and takes a step of 2°C every 5 minutes till the temperature of 50°C is reached. For identification of isotropic materials, it is sufficient to measure the torsion and breathing frequencies on the same test plate (contrary to orthotropic materials for which also the saddle frequency must be measured together with two beam frequencies)

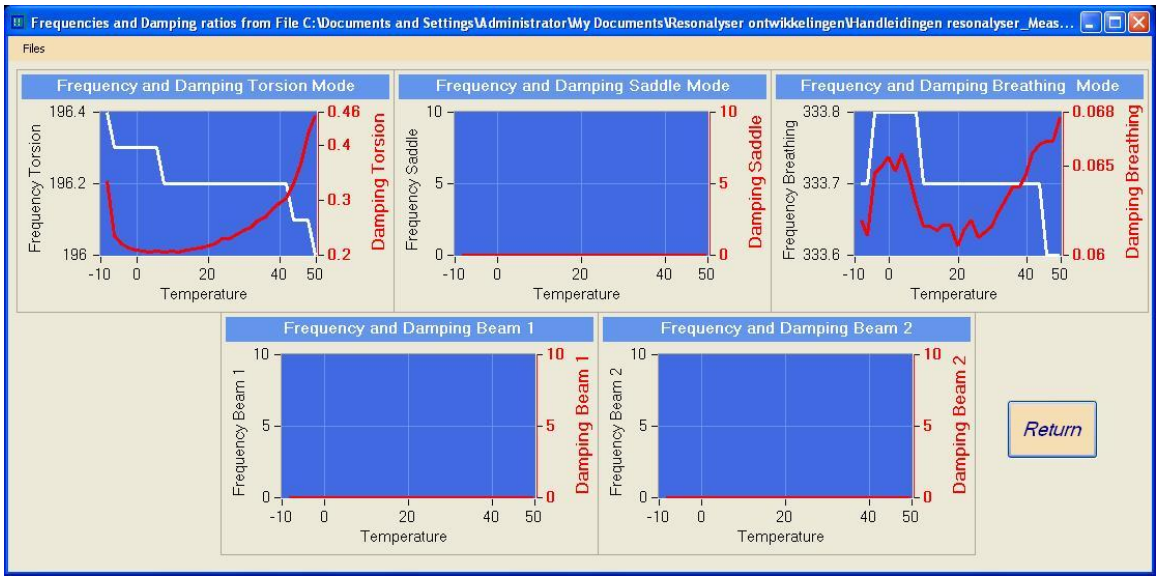

Figure 8.3.1. Measured resonance frequencies and damping ratios.

It can be noticed that the resonance frequency of the torsion modal shape evolves from 196.4 Hz at -10°C towards 196 Hz at 50°C in the zoomed graph. The damping ratio evolves from 0.3 towards 0.46.The resonance frequency of the breathing modal shape evolves from 333.8 Hz at -10°C towards 333.6 Hz at 50°C in the zoomed graph. The damping ratio evolves from 0.06 towards 0.068.The resonalyser software allows the identification of the storage modulus of the Young's modulus E, the Poisson ratio v and the in-plane shear modulus G. The relationship for isotropic materials is:

$$G = \frac{E}{2(1+\nu)} \tag{1}$$

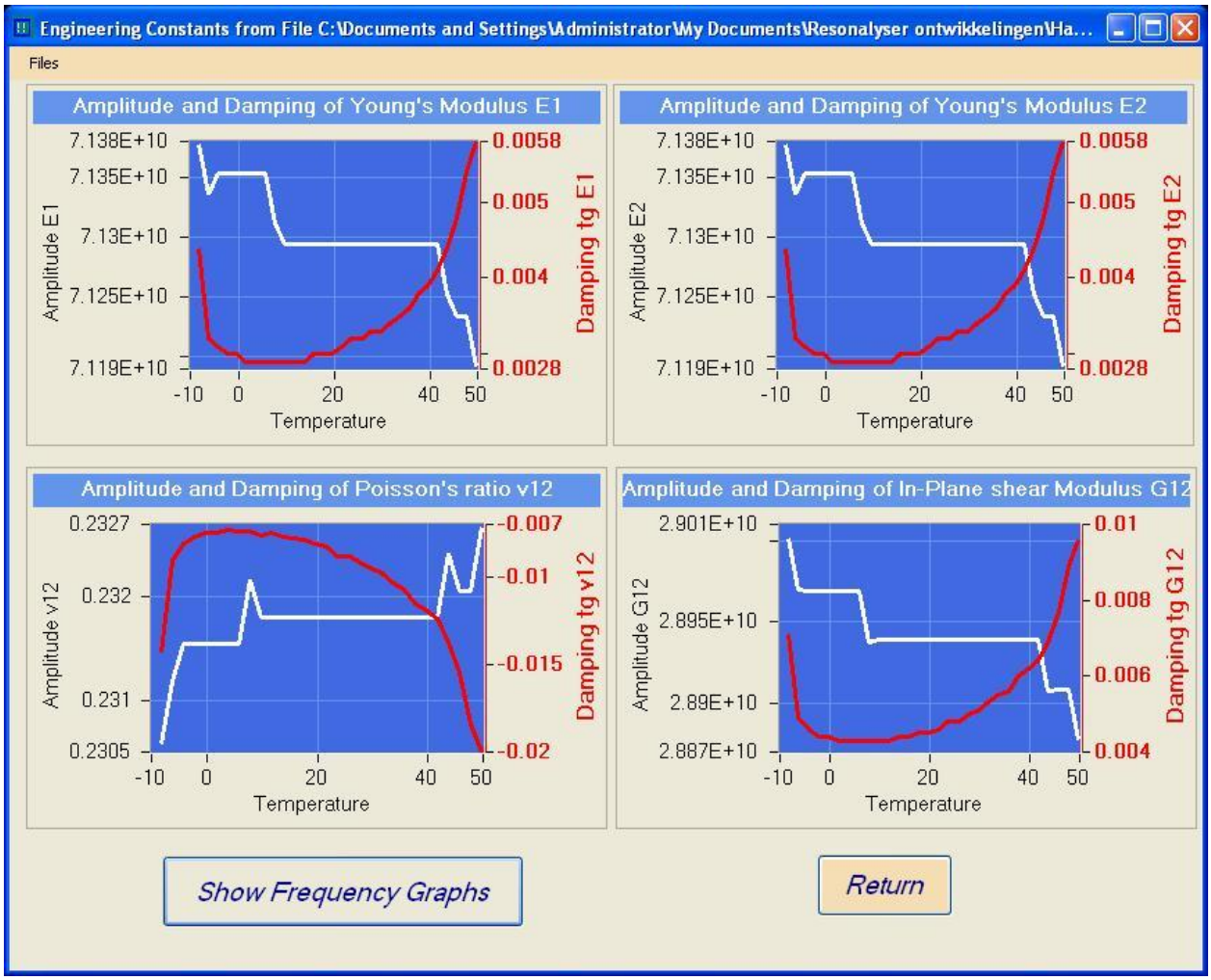

Figure 8.3.2. Identified isotropic engineering constants.

8.3.1 The storage modulus

It can be noticed that the storage values of the engineering constants are constant between 10°C and 40°C.

E = 7.126 E+10
v = 0.232
G = 2.892 E+10

At -10°C, the value of E reaches 7.138 E+10 and at 50°C the value reaches 7.119 E+10.

It can be concluded that the storage modulus of E, v and G can be considered nearly as constant between -10°C and 50°C

8.3.2 The tangents delta

For a sandwich beam, the total potential energy has contributions from the glass and PVB layers.

An expression that derives the contributions of every layer (Potential energy of the bending of both glass layers $PE_{GlassBending}$, the potential energy of the normal force N in the glass layers $PE_{GlassNormalForce}$, the potential energy due to bending of the PVB layer $PE_{PVBBending}$ and the potential energy due to shearing of the PVB layer PE_{PVB}) to the measured damping ratio can be found in [1]:

$$\xi_{Measured} = \frac{1}{2}\left(\frac{PE_{GlassBending}}{TotalPE} tan\,\delta\,(E)_{Glass} + \frac{PE_{GlassNormalForce}}{TotalPE} tan\,\delta\,(E)_{Glass}\right.$$

$$\left. + \frac{PE_{PVBBending}}{TotalPE} tan\,\delta\,(E)_{PVB} + \frac{PE_{PVB}}{TotalPE} tan\,\delta\,(G)_{PVB}\right) \quad (116)$$

It can be seen in figure 8.3.2 that the value of tangents delta of the Young's modulus E varies between 0.0028 and 0.0068.

For the computation of the tangents delta of the PVB only the dissipated energy that originates purely from the shearing behavior of the PVB layer is taken into account the formula reduces to:

$$\xi_{Measured} = \frac{1}{2}\left(\frac{PE_{PVB}}{TotalPE} tan\,\delta\,(G)_{PVB}\right) \quad (117)$$

And:

$$tan\,\delta\,(G)_{PVB} = \frac{Dissipated\ Energy}{2\pi(PE)_{PVB}} = \frac{2\xi_{Measured}}{(PE)_{PVB}/TotalPE} \qquad (118)$$

8.4 Example of identification of the tangents delta of G

To check if the tangents delta of the Young's modulus of the glass can be neglected, the following example will be taken:

Length Beam	:	0.30000 m
Width Beam	:	3.02000E-02 m
Thick skin layer	:	4.94300E-03 m
Thick Poly layer	:	2.24000E-03 m
Specific Mass skin:		2475.0 kg/m3
Specific Mass Poly:		1065.0 kg/m3
Beam Mass	:	0.24329 kg
E-modulus glass	:	7.09000E+10 Pa

With these values, the potential energy distribution is computed:

COMPUTED SANDWICH FREQUENCY:	934.89 Hz
TOTAL POTENTIAL ENERGY:	7.71063E+06
CONTRIBUTION BENDING MOMENT:	1.74185E+06
CONTRIBUTION NORMAL FORCE:	3.58311E+06
CONTRIBUTION SHEAR FORCE:	2.38543E+06
CONTRIBUTION BENDING CORE:	232.02
TOTAL KINETIC ENERGY:	7.71063E+06
CONTRIBUTION MASS:	7.67882E+06
CONTRIBUTION INERTIA:	31806.

The potential energy contribution of the PVB bending can be neglected. The tangents delta for the Young's modulus of glass can be taken as 0.0045. For a measured damping ratio of 2.1234%, the tangents delta can be computed with the complete formula (116) and the simplified formula (118).

$$0.02124 = \frac{1}{2}\left(\frac{1.742E+06}{7.71063E+06}0.0045 + \frac{P3.583E+06}{7.71063E+06}0.0045 + \frac{2.3854E+06}{7.71063E+06}tan\,\delta\,(G)_{PVB}\right) \qquad (116)$$

Thus: $tan\,\delta\,(G)_{PVB}) = 0.127$

$$tan\,\delta\,(G)_{PVB} = \frac{2\xi_{Measured}}{(\frac{PE)_{PVB}}{TotalPE}} = \frac{2x\ 0.021234}{2.3854E+\frac{06}{7.71063E}+06} = 0.137$$

The difference between the tangents delta computed with the full formula (taking the influence of glass damping into account) and with the simplified formula is less than 10%. Considering measurements errors on the damping ratio and the not perfect quality of the test samples, this difference can be neglected.

Ref. [1] Sol, H.; Rahier, H.; Gu, J. Prediction and Measurement of the Damping Ratios of Laminated Polymer Composite Plates. *Materials* **2020**, *13*